Issue No. 40
January 2009

IGACtivities Newsletter

of the International Global Atmospheric Chemistry Project

In this Issue:

Science Features

Announcements

A Note from the IGAC Co-chairs: Kathy Law and Tong Zhu

The IGAC 2008 conference in Annecy, France was a great success with more than 500 attendees. A highlight of the conference was the active engagement of young scientists, who competed in a Young Scientist Poster Contest. At the IGAC 2008 conference, the following five young scientists received the best poster awards:

1. Susannah Burrows, MPI, Mainz, Germany: "Modeling the transport of bacteria as aerosol in the chemistry-climate model ECHAM5/MESSy"

2. Timothy Bertram, Univ. of Washington, Seattle, WA, USA: "Towards in-situ observations of N_2O_5 reactivity"

3. Aldona Wiacek, ETH, Zurich, Switzerland: "Observational constraints on upper tropospheric mineral dust aerosol"

4. Ariela D'Angiola, Atomic Energy National Commission of Argentina & San Martín National University: "Development of new on-road transport emission inventories for the Metropolitan Area of Buenos Aires, Argentina and its spatial disaggregation"

5. Michelle Cain, Univ. of Reading, Reading, U.K.: "Transport and ozone photochemistry in the West African Monsoon region"

These were selected from 83 posters by young scientists, and it was not an easy job for the jury to identify the best among the excellent candidates.

This newsletter includes articles from three of these five Young Scientist poster award winners. In "Direct Observations of N_2O_5 Reactivity", Timothy H. Bertram presents results from the first direct, *in situ* measurements of N_2O_5 reactivity. In "Mineral dust: observations of emission events and modeling of transport to the upper troposphere" Aldona Wiacek et al. explore differences between two mineral dust emission events in the Sahara and one in Asia and the impact that these may have on the availability of mineral dust ice nuclei for interactions with pure ice (cirrus) clouds. In the article by Ariela D'Angiola et al. "Development of spatially disaggregated on-road transport emission inventories for the Metropolitan Area of Buenos Aires, Argentina", a travel-based bottom-up approach was employed for the computation of annual emission inventories of criteria pollutants and greenhouse gases from on-road mobile sources for the year 2006 for the metropolitan area of Buenos Aires, Argentina.

The fourth article of this newsletter is by John Sodeau, summarizing the Lab Studies workshop that took place in June 2007 in Cambridge, U.K. This workshop was a joint endeavor of IGAC and SPARC, and specifically the HitT and AICI Tasks. IGAC and SPARC used to have a joint activity in Lab Studies and we hope the workshop will revitalize this activity. We also hope it will help resolve uncertainties about the role of halogens in determining atmospheric chemical composition and feedbacks with climate (as discussed by vonGlasow in IGACtivities, Issue No. 39) and more generally the issues around Air-Ice Chemical Interactions (see *IGACtivities* Issue No. 29). These and other past issues of *IGACtivities* can be downloaded as pdfs from http://www.igac.noaa.gov/newsletter/index.php.

GLOBAL CHANGE IGBP
A Core Project of the Internations Geosphere-Biosphere Programme

In Cooperation with IAMAS Commission on Atmospheric Chemistry and Global Pollution

Direct Observations of N_2O_5 Reactivity

Contributed by **Timothy H. Bertram** (tbertram@atmos.washington.edu) *and* **Joel A. Thornton** (thornton@atmos.washington.edu) *Department of Atmospheric Sciences; University of Washington, Seattle, WA*

Introduction

Both NO_x ($NO_x \equiv NO+NO_2$) and ozone (O_3) are removed from the atmosphere at night through reactions of N_2O_5 and NO_3 with aerosol particles and volatile organic compounds (VOC), respectively. Our ability to determine the impact of nocturnal NO_x processing on atmospheric oxidants and particle mass loadings continues to be limited by uncertainty in the rates and product branching ratios of the reactions highlighted in Figure 1. Until recently, measurements of NO_3 and N_2O_5 reactivity have been the province of: i) laboratory studies, employing simplified aerosol types and representative VOC to describe functional dependences [Folkers, et al., 2003; Thornton, et al., 2003; Mentel, et al., 1999; Berndt and Boge, 1997], and ii) steady-state analyses using field measurements of NO_3 and N_2O_5 mixing ratios to infer ensemble reaction rates [Aldener, et al., 2006; Brown, et al., 2006]. In this study, we present results from the first direct, in situ measurements of N_2O_5 reactivity. Such measurements provide model-relevant parameters without requiring assumptions about air mass history or extrapolation from idealized laboratory systems. The results we obtained have important implications for the nocturnal processing of NO_x, illustrate the dependence of N_2O_5 reactivity on both particle composition and phase, and provide insights into particulate liquid water content and availability.

Experimental Methods

N_2O_5 reactivity was determined directly on ambient aerosol particles at two sampling locations (Boulder, Colorado, USA and Seattle, Washington, USA) during the summer of 2008. The pseudo-first order rate coefficient for N_2O_5 loss to aerosol particles (k_{het}) was retrieved on a near-hourly basis, using an entrained aerosol flow reactor coupled to a custom-built chemical ionization mass spectrometer (CIMS). Co-located observations of particle surface area (S_a), particle chemical composition, and basic meteorological parameters were used to determine the reactive uptake coefficient (γ) and assess the role of composition and phase in driving variability in the observed N_2O_5 reactivity.

Ambient Observations

Observed values of $\gamma(N_2O_5)$ from the two urban-suburban sampling locations were highly variable, with the reactive uptake coefficient spanning two orders of magnitude ($5x10^{-4} < \gamma < 0.03$). N_2O_5 reactivity was small in regions of low relative humidity (RH<30%, typical of Boulder observations), suggesting that the ambient particles were either crystalline or had very little available liquid water. In contrast, $\gamma(N_2O_5)$ was highly variable at high RH (RH>60%, typical of Seattle observations), illustrating the control of particle chemical composition over N_2O_5 reactivity at higher RH. These results reflect the strong

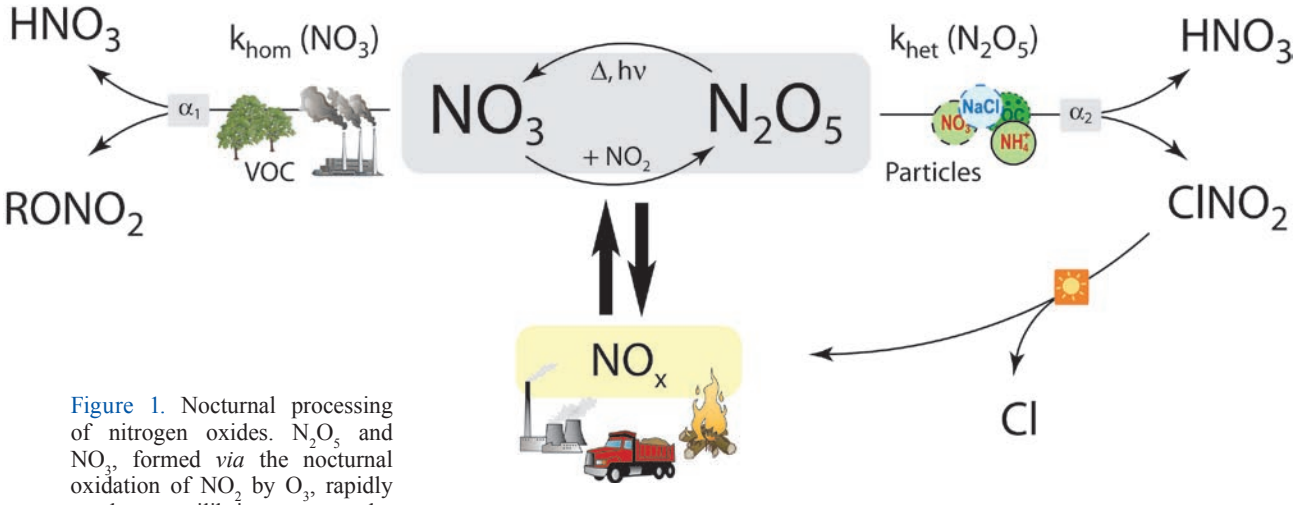

Figure 1. Nocturnal processing of nitrogen oxides. N_2O_5 and NO_3, formed *via* the nocturnal oxidation of NO_2 by O_3, rapidly reach an equilibrium state set by the ambient tempterature and NO_2 mixing ratio. Accurate representation of both the loss rates and product branching ratios for these reactions is critical for describing the effect of nocturnal nitrogen processing on oxidant concentrations and particle mass loadings.

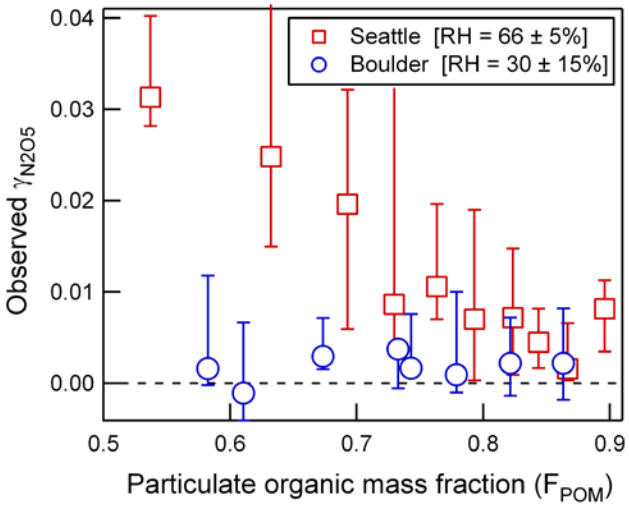

Figure 2. Observed dependence of g(N2O5) on the particulate organic mass fraction for measurements made in Boulder, CO (blue circles, 3-21 July 2008) and Seattle, WA (red squares, 6-16 August 2008). Data points are equal population binned medians; the error bars represent the interquartile range of the observations.

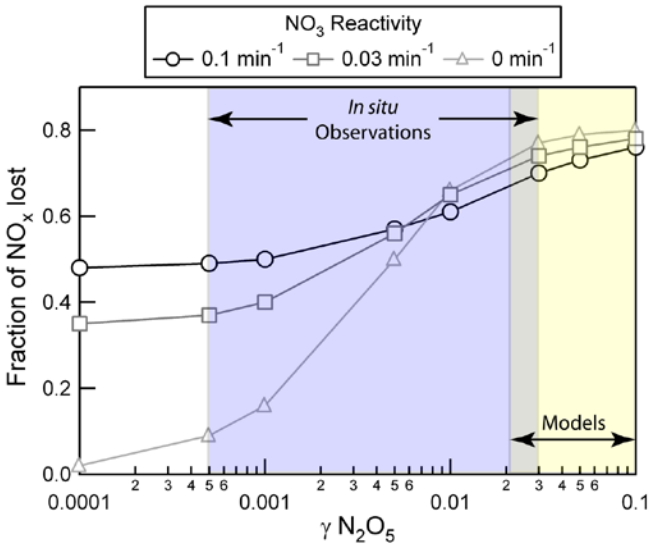

FIgure 3. Fraction of available NO_x ($[NO_x]_{sunset}$) lost during a 12-hr night as a function of $\gamma(N_2O_5)$ and NO_3 reactivity (0-0.1 min^{-1}). Values were calculated using a time-dependent chemical box model, with the following initial conditions: temperature = 298°K, $[O_3]$ = 40 ppbv, $[NO_2]$ = 10 ppbv, and S_a = 200 $\mu m^2 cm^{-3}$. The blue shaded region represents the variability in the observed $\gamma(N_2O_5)$ in Seattle, WA and the yellow shaded region depicts the range in $\gamma(N_2O_5)$ captured by the current generation of chemical transport models.

dependence of $\gamma(N_2O_5)$ on particle liquid water content. As shown in Figure 2, comparison with ambient observations of particle chemical composition reveal a strong, inverse relationship between $\gamma(N_2O_5)$ and particulate organic matter mass fraction (F_{POM}). The observed dependence of $\gamma(N_2O_5)$ on F_{POM} at high RH can be hypothesized to be a result of: i) an increase in the fraction of externally mixed hydrophobic organic particles, ii) a decrease in the liquid water mass fraction of internally mixed particles following increased partitioning of hydrophobic organics to existing particles, iii) an increasing role of organic coatings that limit either N_2O_5 surface accommodation or N_2O_5 accessibility to particle liquid water or iv) some combination of all of the above. Further discussion of the role of particle chemical composition and phase in determining $\gamma(N_2O_5)$ can be found in Bertram et al. [2008], submitted to *Geophysical Research Letters*.

Atmospheric Implications

The current generation of regional and global chemistry models parameterize $\gamma(N_2O_5)$ using the existing suite of laboratory measurements [*Evans and Jacob*, 2005; *Riemer, et al.*, 2003; *Dentener and Crutzen*, 1993]. Due to the complexity in the organic component of ambient particles, parameterizations based on a relatively small set of organic surrogates may not accurately represent atmospheric conditions. The observations presented here imply that organic material found in particles near their source region is largely hydrophobic, acting to limit liquid water availability and suppress $\gamma(N_2O_5)$. The fraction of NO_x removed during the course of a single night will be sensitive to $\gamma(N_2O_5)$, particle loadings and NO_3 reactivity, as we illustrate with the output of a time-dependent box model simulation (Figure 3). For the conditions sampled in Seattle, these simulations show that current model parameterizations overestimate $\gamma(N_2O_5)$ and that modeled NO_x will be sensitive to the changes in $\gamma(N_2O_5)$ required to match values suggested by our observations. Future ambient observations of N_2O_5 reactivity outside of near-source regions will be instructive in the development of robust parameterizations for $\gamma(N_2O_5)$ that will ultimately refine the representation of the nocturnal NO_x lifetime in chemical transport models. If the results presented here prove to be a general description for the role of organics in controlling $\gamma(N_2O_5)$, we can expect that the NO_x lifetime in most models will be extended, having consequent effects on the rate of tropospheric O_3 production. Further, these results imply that the NO_x lifetime will be more strongly dependent on the modeled NO_3 reactivity.

Acknowledgments

This work was funded in part by a grant from the Office of Earth Science (NIP/03-0000-0025) at the National Aeronautics and Space Administration. THB gratefully acknowledges the NOAA Climate and Global Change Fellowship Program for financial support. We thank Ann M. Middlebrook, Roya Bahreini, and Charles Brock (NOAA ESRL) for particle measurements during NORAA-Boulder and Timothy S. Bates, Patricia K. Quinn, and Derek J. Coffman (NOAA PMEL) for particle measurements during NORAA-Seattle. The work described here has been submitted for publication in *Geophysical Research Letters*.

References

Aldener, M., et al. Reactivity and loss mechanisms of NO_3 and N_2O_5 in a polluted marine environment: Results from in situ measurements during New England Air Quality Study 2002, *J. Geophys. Res.*, **111(D23)**, 2006.

Berndt, T., and O. Boge. Products and mechanism of the gas-phase reaction of NO_3 radicals with alpha-pinene. *J. Chem. Soc.-Faraday Transac.*, **93(17)**, 3021-3027, 1997.

Brown, S. S., et al. Variability in nocturnal nitrogen oxide processing and its role in regional air quality, *Science*, **311(5757)**, 67-70, 2006.
Dentener, F. J., and P. J. Crutzen. Reaction of N_2O_5 on Tropospheric Aerosols - Impact on the Global Distributions of NO_x, O_3, and OH, *J. Geophys. Res.*, **98(D4)**, 7149-7163,1993.
Evans, M. J., and D. J. Jacob. Impact of new laboratory studies of N_2O_5 hydrolysis on global model budgets of tropospheric nitrogen oxides, ozone, and OH, *Geophys. Res. Let.*, **32 (9)**, 2005.
Folkers, M., et al. Influence of an organic coating on the reactivity of aqueous aerosols probed by the heterogeneous hydrolysis of N_2O_5, *Geophys. Res. Let.*, **30(12)**, 2003.
Mentel, T. F., et al. Nitrate effect in the heterogeneous hydrolysis of dinitrogen pentoxide on aqueous aerosols, *Phys. Chem. Chem. Phys.*, **1(24)**, 5451-5457, 1999.
Riemer, N., et al., Impact of the heterogeneous hydrolysis of N_2O_5 on chemistry and nitrate aerosol formation in the lower troposphere under photosmog conditions, *J. Geophys. Res.*, **108 (D4)**, 2003.
Thornton, J. A., et al. N_2O_5 hydrolysis on sub-micron organic aerosols: the effect of relative humidity, particle phase, and particle size, *Phys. Chem. Chem. Phys.*, **5(20)**, 4593-4603, 2003.

Mineral dust: observations of emission events and modeling of transport to the upper troposphere

Contributed by **Aldona Wiacek** (aldona.wiacek@Dal.Ca), **Michael Taddeo** (mtaddeo@student.ethz.ch) *and* **Thomas Peter** (thomas.peter@env.ethz.ch), *Institute for Atmospheric and Climate Science, ETH, Zürich, Switzerland*

Introduction

Naturally occurring mineral dust is, on a mass basis, the most abundant aerosol in the atmosphere (*Satheesh and Moorthy, 2005*). Emitted every few days in large quantities from sources in the Sahara in the summer, and from sources in Asia in the spring, it travels great distances westward across the Atlantic and eastward across the Pacific, respectively (*e.g., Miller et al., 2006*).

Along its journey, it is known to fertilize the oceans with nutrients and in this way it has feedbacks on the carbon cycle (*Tegen, 2003*). These dust plumes also have a strong direct radiative aerosol effect, which feeds back on surface temperatures and winds, as well as on climate. The direct radiative effects of African dust have been the focus of several recent measurement campaigns, including SAMUM[1], DODO[2] and DABEX[3]. However, one of the biggest uncertainties related to aerosols in general and mineral dust in particular, is their indirect radiative effect, i.e., how they affect cloud reflectivity and lifetime, as well as their effect on the precipitating properties of clouds (*Forster et al., 2007*). For example, there is now increasing evidence that the ubiquitous layer of mineral dust found over the tropical Atlantic during the summer is linked to hurricane formation processes and hurricane intensity (*e.g., Dunion and Velden, 2004; Wu, 2007*).

Analysis of TRMM[4] data reveals that cold rain processes account for more than two thirds of the total rain amount in the tropics (*Lau and Wu, 2003*). These processes involve the ice phase as intermediate state. This ice may occur at high altitudes in cold cirrus clouds or at intermediate altitudes in ice or mixed-phase clouds containing an external mixture of ice crystals and supercooled water droplets. In the mixed-phase or low ice clouds nucleation of ice cannot occur homogeneously, requiring ice nuclei to initiate heterogeneous nucleation. It has been known for a long time that mineral dust particles may be efficient ice nuclei (IN) (*Mason and Maybank, 1958; DeMott et al., 2003a*) and recent aircraft-based single-particle measurements find evidence of mineral dust in ice crystal residuals (*e.g. DeMott et al., 2003b*). Additionally, polarization LIDAR measurements provide further evidence for both African and Asian dust causing the glaciation of supercooled water clouds at a range of temperatures (*Sassen, 2002; Sassen et al., 2003; Ansmann et al., 2005, 2008*). However, uncertainties in this aerosol's atmospheric lifecycle are very large (*Textor et al., 2006; Cakmur et al., 2006*) thus introducing corresponding uncertainties in quantitative estimates of the impact of mineral dust on the ice phase of clouds and precipitation in global models (*e.g., Hoose et al., 2008; Storelvmo et al., 2008*).

The Saharan dust source accounts for nearly two thirds of the total mass of global dust emissions, and, to first order, Asian dust sources make up the balance (*Satheesh and Moorthy, 2005*). On account of its low source latitude (15-30° N) Saharan dust is transported

[1]SAharan Mineral dUst experiMent, http://samum.tropos.de/scopeover.html

[2]Dust Outflow and Deposition to the Ocean, http://badc.nerc.ac.uk/data/solas/projects/dodo.html

[3]Dust And Biomass EXperiment, http://badc.nerc.ac.uk/data/dabex/

[4]Tropical Rainfall Measuring Mission, http://trmm.gsfc.nasa.gov/

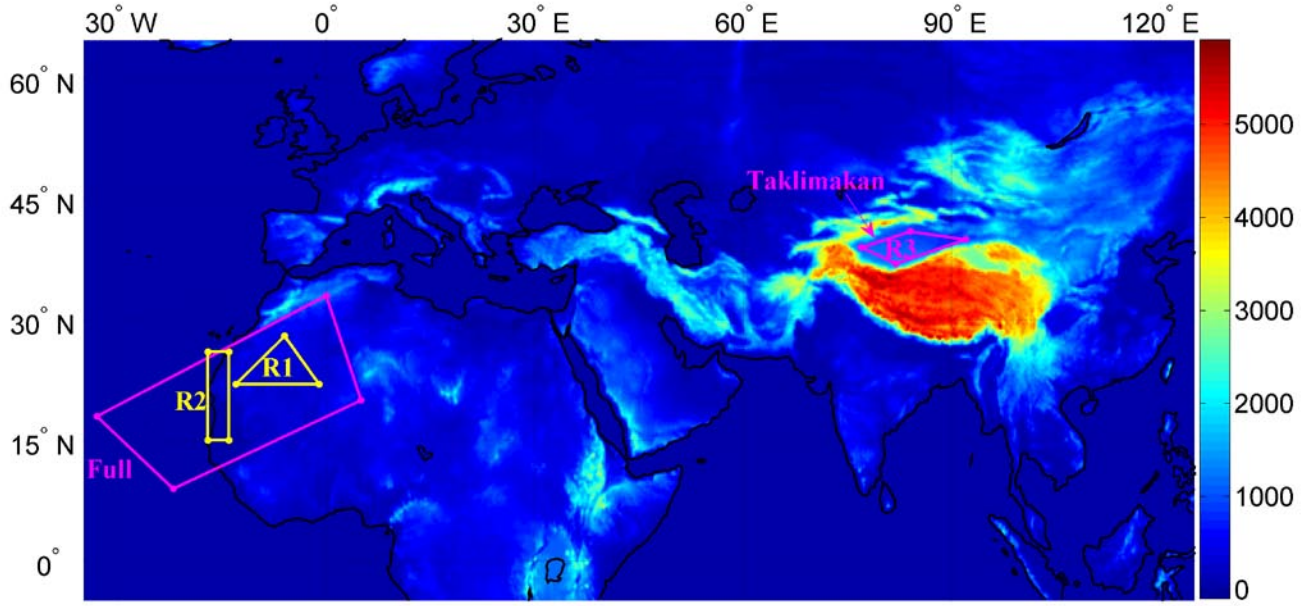

Figure 1 Partial world topography, as represented in the T799 resolution (0.225°) ECMWF general circulation model, showing the African and Asian regions used in the forward trajectory calculations for the respective case studies. The colorbar shows the terrain altitude in meters.

westwards across the Atlantic, while Asian dust, which is sourced between 30-50° N, is transported eastwards across the Pacific. Although Asian dust sources comprise the Taklimakan and Gobi deserts, we focus on the former, as dust from the Gobi desert is thought to be confined to < 3 km altitude 90% of the time. However, dust from the Taklimakan desert (found within the Tarim Basin) is entrained relatively easily to > 5 km (*Sun et al., 2001*), partly due to the complex surrounding topography (Figure 1).

The present study explores differences between two mineral dust emission events in the Sahara and one in Asia, and the impact that these may have on the availability of mineral dust ice nuclei (IN) for interactions with pure ice (cirrus) clouds.

Method

The approach taken was to perform trajectory-based case studies of dust emission events in both desert regions using a combination of active (CALIPSO[5]) and passive (OMI[6]) satellite observations, as well as a dust emission model (NAAPS[7]). Forward trajectory calculations were started from domains of high dust concentration as shown by the satellite measurements and model simulations (in close proximity to, but not exactly coincident with, known dust source regions). The ascent of trajectories was evaluated along with the air's temperature (T) and relative humidity with respect to water (RH_w) and ice (RH_i), as these are known from laboratory studies to affect the activity of IN. We also diagnosed local cloud liquid and ice water content (LWC, IWC) and equivalent potential temperature (θ_e), although these variables are not discussed herein.

All trajectories were calculated using the LAGRangian trajectory ANalysis TOol (LAGRANTO) developed by Wernli and Davies (*1997*). In order to better capture the complex wind patterns in Asia's Taklimakan desert, which is surrounded by the extremely rugged topography of the Tarim Basin margin (Figure 1), we employed the highest resolution wind fields available operationally at present. These are T799 / ~0.225° horizontal resolution analyses available at 00Z, 06Z, 12Z and 18Z from the European Centre for Medium-range Weather Forecasts (ECWMF). The ECMWF model uses a hybrid coordinate system that follows the terrain near the surface and relaxes to horizontal surfaces in higher model layers; there are ~50 model levels in the troposphere alone (*Untch et al., 2006*).

The relative humidity with respect to water and ice was calculated in a Lagrangian manner by subjecting the relative humidity from the initial trajectory time (t = 0) to pressure and temperature values at all future times in the trajectory. The advantage of this approach is that we were able to decouple from the treatment of water condensation and ice nucleation employed in the ECMWF model. In particular, we were able to simulate conditions of ice supersaturation along our trajectories, which are not represented in ECMWF analyses fields. However, the quality of assimilated fields in remote regions with few observations can always be questioned. In the case of the Taklimakan desert in the Tarim Basin, we compared the surface values of T and RH in the ECMWF model with ground-based station data (Tazhong Station 39.0°N, 83.67°E, 1100 m asl) and found very

[5]Cloud-Aerosol Lidar and Infrared Pathfinder Satellite Observation, http://www-calipso.larc.nasa.gov/

[6]Ozone Monitoring Instrument, http://www.knmi.nl/omi

[7]Navy Aerosol Analysis and Prediction System, http://www.nrlmry.navy.mil/aerosol_web/Docs/globaer_model.html

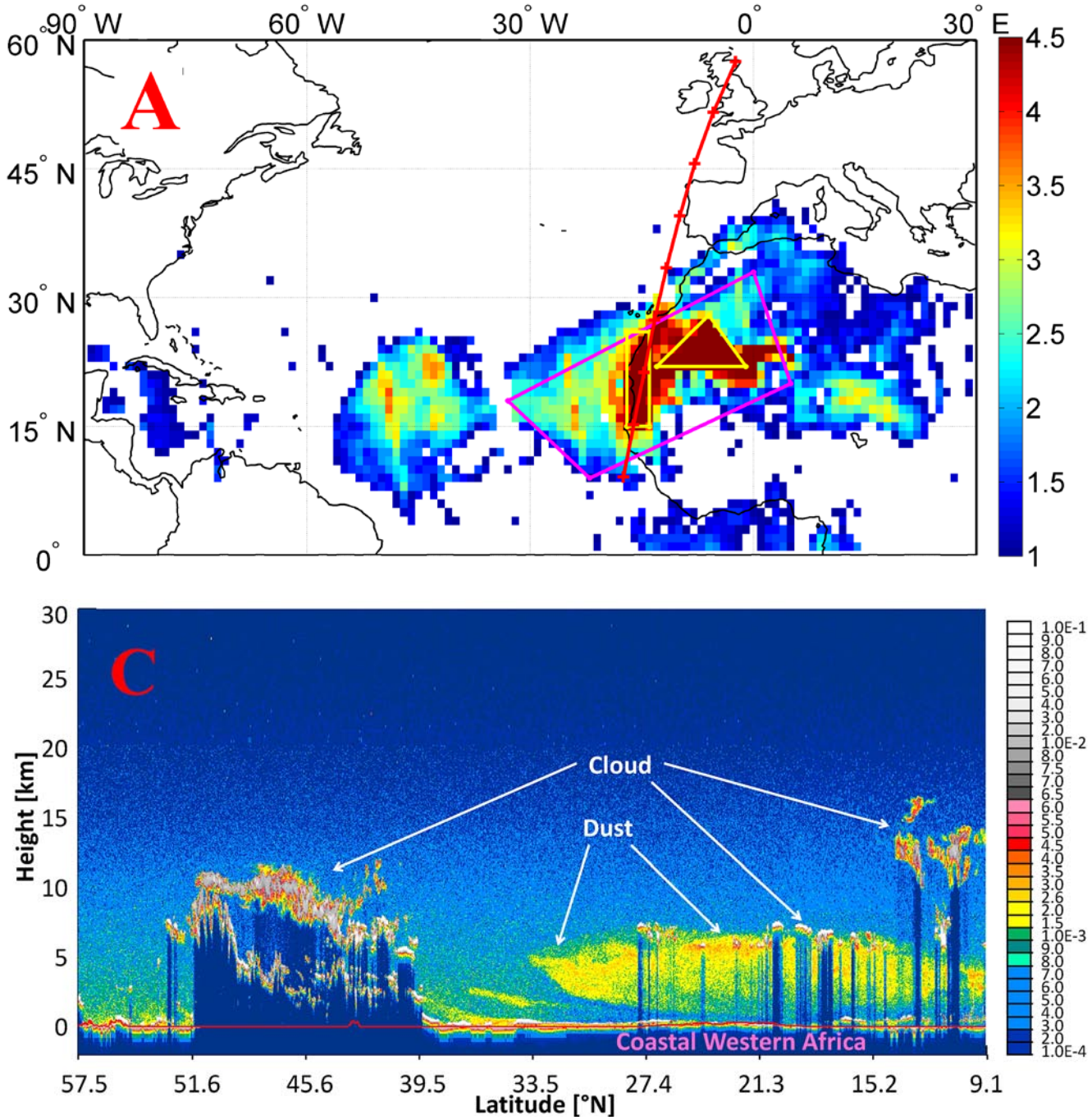

Figure 2 Panels A and B show the Level 3 Aerosol Index measured during strong dust emission events by the OMI satellite instrument over the Sahara (Jul-15-2007) and over the Tarim basin (May-20-2007). The AI values are set to saturate at 4.5. Boundaries of trajectory calculation regions are shown as in Figure 1, while the near-vertical red lines indicate the location of same-day, night-time CALIPSO satellite instrument measurements, which are shown in Panels C and D. The CALIPSO data (version 2.01) shows total attenuated backscatter [$km^{-1}sr^{-1}$] at 532 nm as a function of height [km] approximately from north to south (left to right), as indicated by the red lines in Panels A and B. The thin horizontal red line in Panels C and D shows the topography.

good agreement throughout the year.

A drawback of our approach is that we neglect mixing processes in the "transported" or "Lagrangian" relative humidities. However, the wind-blown dust from the Tazhong region often rises in parcels of very hot and dry air – e.g. 30°C and 4% RH – so that mixing with air from the less arid regions surrounding the Taklimakan will mostly result in a moistening effect. Hence, as long as we are predominantly interested in whether the dust has any chance to reach the 0°C-level without undergoing previous processing or washout by cloud drop formation, the no-mixing assumption is a justified and conservative simplification.

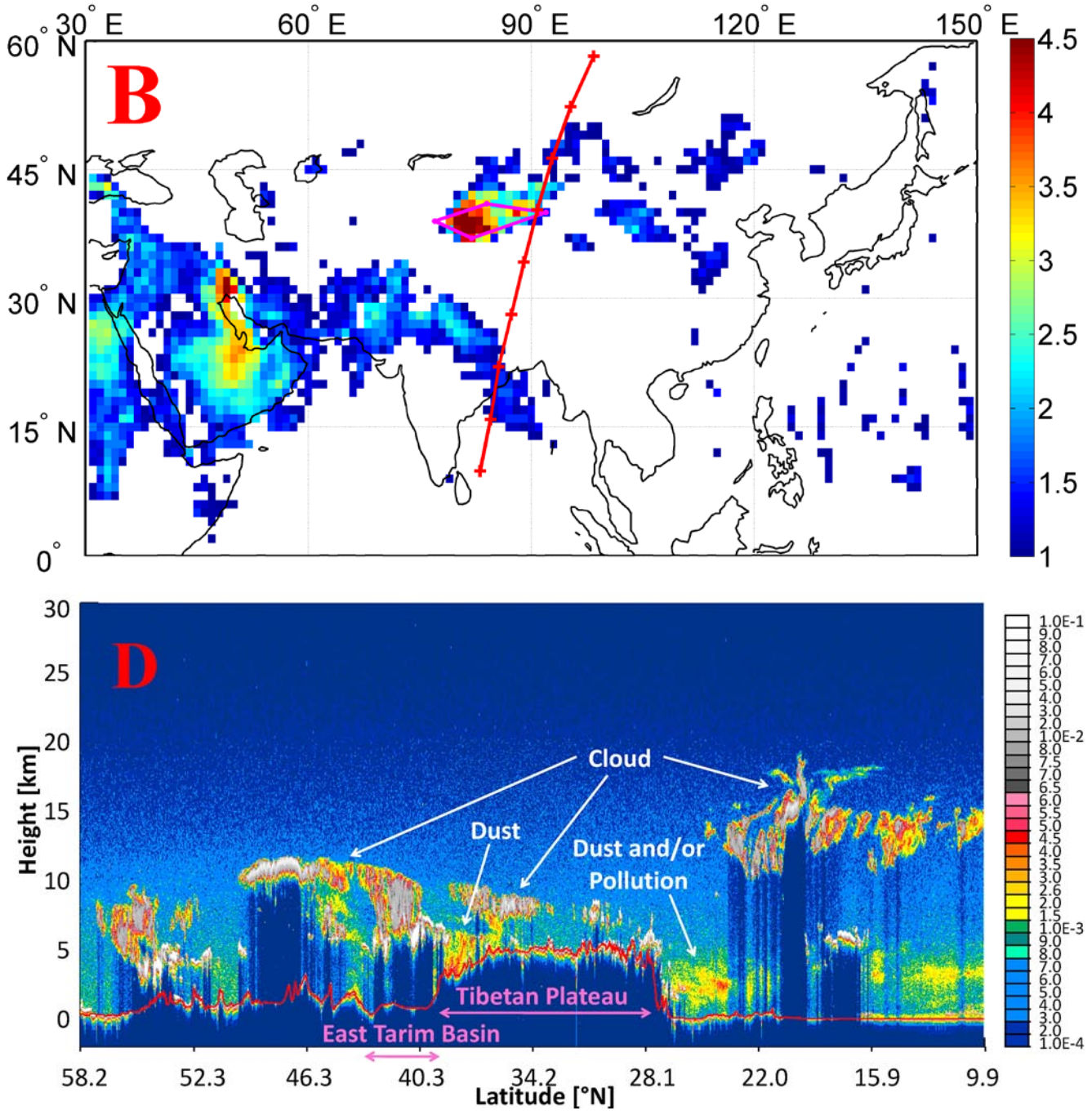

Figure 2 Continued.

Case Studies

Dust activity is very strong in the summer months in Africa and in the spring months in Asia. As such we were able to find an intense dust emission event in West Africa on July 15th, 2007, and one in the Taklimakan desert on May 20th, 2007. The events manifest themselves as an increased aerosol index in the OMI satellite measurements (Figure 2). Given the location and season, it is very unlikely that the signal is due to other absorbing aerosols; nonetheless, we confirmed that dust emission was also predicted with the NAAPS model (not shown). The vertical dimension of the dust emissions is revealed in the CALIPSO satellite measurements of total attenuated backscatter, also shown in Figure 2. The African plume is ~5 km thick over nearly its entire latitudinal extent from ~30°N to ~15°N. Regions of total or near-total extinction of the CALIPSO lidar signal manifest as dark blue vertical stripes underneath thin and scattered water clouds (regions of strong backscatter shaded grey-white in Figure 2, panels C and D). On May 20th, the Taklimakan plume is obstructed by clouds except at the southern margins of the Tarim Basin, already on the northern slopes of the Tibetan Plateau. Nonetheless, we chose this event because of additional

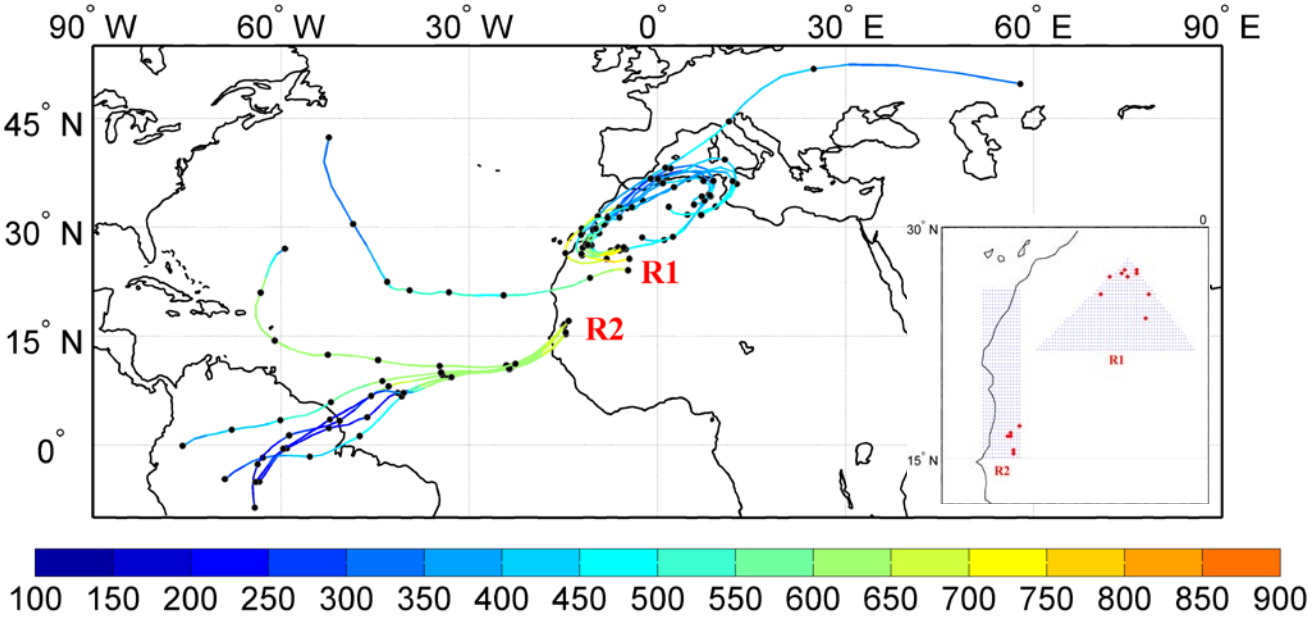

Figure 3 Trajectories started from African plume regions R1 and R2 that ascended from 700 mb to 450 mb (1.1% of all trajectories). The inset shows their starting coordinates as red points set among a grid showing all trajectory starting points (small blue dots). The black dots in the main figure indicate the trajectory location at 24 hour intervals and the color along a trajectory indicates its pressure (mb).

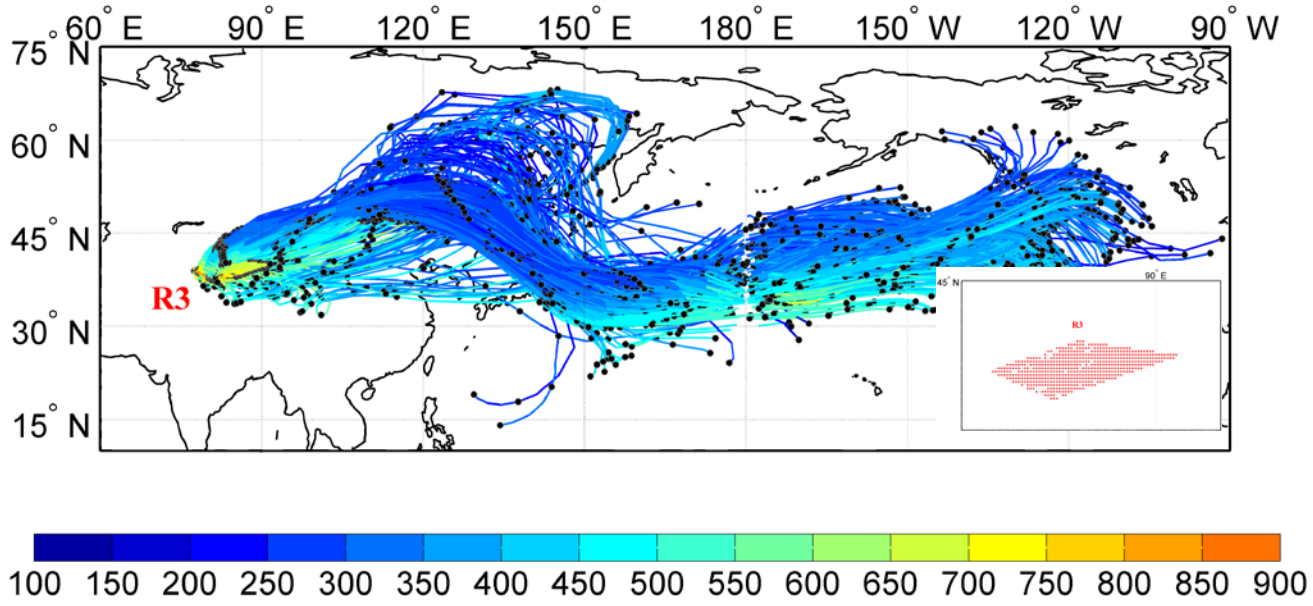

Figure 4. As in Figure 3, but for trajectories started from the Asian plume region R3 which ascended from 700 mb to 450 mb (93% of all trajectories).

OMI and CALIPSO observations, NAAPS model simulations and our own trajectory calculations (not shown), which provide further evidence that a strong dust emission event is taking place.

One-week (168 hr) forward trajectories were calculated by filling the domains indicated in Figure 1 with uniformly distributed trajectories every 0.225°. This resulted in 8575 trajectories for the entire African region, 729 trajectories for African region R1 and 637 trajectories for African region R2, both focusing on zones of high aerosol index observations indicated by the OMI satellite. A comparable set of 570 trajectories was generated for the single Taklimakan region R3. Calculations in each horizontal plane were carried out at pressures of 600, 700 and 800 mb, as well as at two times, 00Z and 12Z. Figure 3 shows African

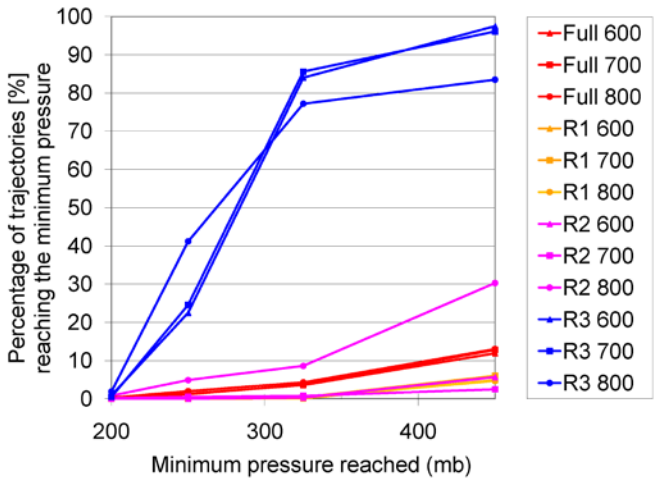

Figure 5 The percentage of trajectories from different regions (R1, R2, R3 and Full, as shown in Figure 1) and starting pressures that ascended to various minimum pressure (or maximum height) criteria; the abbreviations in the legend refer to region name and starting pressure (600, 700 or 800 mb).

trajectories from R1 and R2 that started from the 700 mb plane and fulfilled the criterion of ascent to 450 mb, which corresponds to altitudes ≥ 6 km. Only 1.1% of trajectories experienced such ascent, and their starting locations are shown as red dots in the inset panel. Figure 4 shows Asian trajectories started from the 700 mb plane in the Taklimakan region R3, which also fulfilled the criterion of ascent to 450 mb. In stark contrast to Africa, 93% of trajectories experienced such ascent.

A pressure of 700 mb was the chosen starting pressure because it falls in the middle of the African dust plume and it is also firmly above the topography of the Tarim Basin (900-1500 m); however, the trajectory simulations were also repeated in all regions at starting pressures of 800 mb (very close to the surface of the Tarim Basin) and 600 mb. In all cases, the Asian trajectories experienced considerably more ascent than the African trajectories, as summarized in Figure 5. We tested for ascent to various minimum pressures (maximum heights) and found that even when the criterion was an ascent to 250 mb (≥ 10 km), the Asian trajectories experienced ~20% more ascent than the African trajectories. Finally, all calculations were also repeated for trajectories starting from 12Z and the results remain very similar.

The reason for these differences in ascent is likely a combination of three factors: First, the complex topography surrounding the Taklimakan Desert, which under easterly winds forces the dust-laden air upwards at the solid walls of the south-west margins of the Tarim Basin (see Figure 1). Second, the overall higher elevation of the Taklimakan Desert (900 m at the Eastern rim near 90°E to 1500 m at the western rim near 75°E) versus the West African dust source (less than a few hundred meters), which implies that the Taklimakan desert reaches surface potential temperatures similar to those over Africa, even though the Sahara is a much hotter desert. Third, and probably most important, upon adiabatic ascent, the surface potential temperature values in question (~300-320 K) climatologically correspond to higher altitudes at mid-latitudes than in the tropics.

While assessing the relative importance of these three factors in dust lifting is beyond the scope of this study, we did examine other variables along the ascending trajectory paths in order to understand better the role of dust aerosol as IN. In particular, we tested the trajectories for conditions in which cirrus clouds could exist in isolation from mixed-phase clouds, i.e. where $RH_w < 100\%$ and $RH_i > 100\%$. Furthermore, we looked at two temperature ranges separately: $T < -35°C$ and $-35°C < T < 0°C$. In the first range, temperatures are low enough that ice can nucleate homogeneously via the spontaneous freezing of liquid-only droplets (provided they consist of pure water or sufficiently dilute solutions). The second temperature range is too warm for homogeneous nucleation; however, ice can nucleate heterogeneously, i.e. via the freezing of droplets of pure water or liquid solutions that contain a solid immersion such as a mineral dust particle (*e.g. DeMott et al., 2003a*).

Based on trajectory simulations originating from 600, 700 and 800 mb at both 00Z and 12Z and from both the Taklimakan (R3) as well as West Africa (R1 and R2), we find that no trajectories ever reach temperatures colder than -35°C prior to achieving water saturation. Although the true relative humidities found along the transport trajectories will be influenced by both mixing and condensation, which we do not model explicitly, we can cautiously conclude that mineral dust aerosols are unlikely to play a significant role in ice nucleation at homogeneous freezing temperatures. It is likely that over the Sahara some re-release of IN at convective outflow levels is taking place, however, these IN would be heavily processed, and as such are not the focus of our study. Concerning the temperature range from $-35°C < T < 0°C$, we find that on average, 2.9% of Taklimakan R3 trajectory points (where the total points are the number of trajectories multiplied by number of points in each trajectory) meet the criterion of supersaturation with respect to ice while not having reached water saturation. Trajectories originating from West African regions R1 and R2 meet the same criteria, on average, 0.5% and 0.8% of the time, respectively. The implication of this is that, if our cases are representative beyond the two episodes presented so far, the much smaller Taklimakan Desert may be a more important source of uncoated ice nuclei than the West African dust sources, which emit much more dust mass in total. Further trajectory studies of a statistical nature, which are the subject of a forthcoming publication, indicate that this is indeed the case.

Summary

The present study explored differences between mineral dust emission events in West African and Asian (Taklimakan) deserts, focusing on the availability of bare mineral dust ice nuclei for interactions with cirrus clouds without previous processing or washout by liquid water clouds. One-week trajectory calculations with high-resolution ECMWF fields were used to track transported (Lagrangian) relative humidities with respect to water and ice at temperatures below 0°C for two case studies in May (Asia) and July (Africa) of 2007. Transport trajectories can reasonably be assumed to carry dust with them throughout the year, except for the months of December-February, which are quiescent with respect to dust emission in both regions. None of the simulated air parcels reach regions where homogeneous nucleation can take place ($T < -35°C$) along trajectories that have not experienced water saturation first, i.e. it is very unlikely that mineral dust particles could be a serious competitor for homogeneous nucleation during the formation of high, cold cirrus clouds. For the temperature region between $-35°C < T < 0°C$, i.e. in air parcels exhibiting necessary conditions for warmer ice clouds at lower altitudes, a small but significant number of air parcels are found to follow trajectories where $RH_w < 100\%$ and $RH_i > 100\%$ are simultaneously maintained. However, the potential for such low ice clouds originating from the Taklimakan desert is greater than that of the Sahara by a factor of 4-6 in the case studies presented in this work. The implication is that although the Sahara is by far the biggest source of dust in the world, the much smaller Taklimakan desert in China's Tarim Basin may be of greater importance as a source of ice nuclei affecting cirrus cloud formation. This is likely the result of several meteorological factors, including the complex regional topography combined with the higher altitude of Taklimakan dust emissions and, on the synoptic scale, the higher altitude of potential temperature levels in the free troposphere at mid-latitudes than in the tropics.

The representativeness of the case studies presented in this work has been established more firmly through a comprehensive trajectory analysis study of a statistical nature from the West African and Taklimakan dust source regions for the entire year 2007. Furthermore, the very active Bodélé source region in Africa and the Gobi Desert in Asia were also examined. Finally, an analysis of the potential availability of mineral dust has been carried out in mixed-phase as well as warm cloud regions, and is the subject of a publication currently in preparation.

Acknowledgments

This work makes extensive use of OMI and CALIPSO satellite data generously made available by NASA, NAAPS dust model outputs made available by the U.S. Naval Research Laboratory, ECMWF analyses, and the LAGRANTO trajectory analysis tool developed by Prof. Heini Wernli while at ETH. We thank Dr. Dominik Brunner from Empa (Switzerland) for providing an introduction to LAGRANTO modeling and Dr. Michael Sprenger from ETH (Switzerland) for providing assistance with FORTRAN and Matlab programming. This work was supported by a Marie Curie Incoming International Fellowship awarded by the European Commission under Framework Programme 6.

References

Ansmann, A., I. Mattis, D. Müller, U. Wandinger, M. Radlach, D. Althausen, and R. Damoah, Ice formation in Saharan dust over central Europe observed with temperature/humidity/aerosol Raman lidar, *J. Geophys. Res.*, **110**, D18S12, doi:10.1029/2004JD005000, 2005.

Ansmann, A., et al., Influence of Saharan dust on cloud glaciation in southern Morocco during the Saharan Mineral Dust Experiment, J. Geophys. Res., 113, D04210, doi:10.1029/2007JD008785, 2008.

Cakmur, R. V., R. L. Miller, J. Perlwitz, I. V. Geogdzhayev, P. Ginoux, D. Koch, K. E. Kohfeld, I. Tegen, and C. S. Zender, Constraining the magnitude of the global dust cycle by minimizing the difference between a model and observations, *J. Geophys. Res.*, **111**, D06207, doi:10.1029/2005JD005791, 2006.

DeMott, P. J., D. J. Cziczo, A. J. Prenni, D. M. Murphy, S. M. Kreidenweis, D. S. Thomson, R. Borys, and D. C. Rogers, Measurements of the concentration and composition of nuclei for cirrus formation, *Proc. Natl. Acad. Sci.*, **100**, 14655-14660, doi:10.1073/pnas.2532677100, 2003a.

DeMott, P. J., K. Sassen, M. R. Poellot, D. Baumgardner, D. C. Rogers, S. D. Brooks, A. J. Prenni, and S. M. Kreidenweis, African dust aerosols as atmospheric ice nuclei, *Geophys. Res. Lett.*, 30(14), 1732, doi:10.1029/2003GL017410, 2003b.

Dunion, L. P. and C. S. Velden, The Impact of the Saharan Air Layer on Atlantic Tropical Cyclone Activity, *Bull. Amer. Meteor. Soc.*, **85**, 353–365, 2004.

Forster, P., et al., Changes in Atmospheric Constituents and in Radiative Forcing. *In: Climate Change 2007: The Physical Science Basis. Contribution of Working Group I to the Fourth Assessment Report of the IPCC* [Solomon, S., D. Qin, M. Manning, Z. Chen, M. Marquis, K.B. Averyt, M.Tignor and H.L. Miller (eds.)]. Cambridge University Press, Cambridge, United Kingdom and New York, NY, USA, 2007.

Hoose, C., U. Lohmann, R. Erdin, and I. Tegen, The global influence of dust mineralogical composition on heterogeneous ice nucleation in mixed-phase clouds, *Environ. Res. Lett.*, **3**, doi:10.1088/1748-9326/3/2/025003, 2008.

Lau, K. M. and H. T. Wu, Warm rain processes over tropical oceans and climate implications, *Geophys. Res. Lett.*, **30**(24), 2290, doi:10.1029/2003GL018567, 2003.

Mason, B. J., and J. Maybank, Ice-nucleating properties of some natural mineral dusts, *Q. J. R. Meteorol. Soc.*, **84**, 235– 241, 1958.

Miller, R. L., et al., Mineral dust aerosols in the NASA Goddard Institute for Space Sciences ModelE atmospheric general circulation model, *J. Geophys. Res.*, **111**, D06208, doi:10.1029/2005JD005796, 2006.

Sassen, K., Indirect climate forcing over the western US from Asian dust storms, *Geophys. Res. Lett.*, **29**(10), 1465, doi:10.1029/2001GL014051, 2002.

Sassen, K., P. J. DeMott, J. M. Prospero, and M. R. Poellot, Saharan dust storms and indirect aerosol effects on clouds: CRYSTAL-FACE results, *Geophys. Res. Lett.*, **30**(12), 1633, doi:10.1029/2003GL017371, 2003.

Satheesh, S.K. and K.K. Moorthy, Radiative effects of natural aerosols: A review, *Atm. Env.*, **39**, 2089 – 2110, doi:10.1016/j.atmosenv.2004.12.029, 2005.

Storelvmo, T., J.E. Kristjánsson, and U. Lohmann, Aerosol Influence on Mixed-Phase Clouds in CAM-Oslo. *J. Atmos. Sci.*, **65**, 3214–3230, 2008.

Sun, J., Zhang M., and T. Liu, Spatial and temporal characteristics of dust storms in China and its surrounding regions, 1960-1999: Relations to source area and climate, *J. Geophys. Res.*, **106**, D10, 10325-10333, 2001.

Textor, C. et al., Analysis and quantification of the diversities of aerosol life cycles within AeroCom, *Atm. Chem. Phys.*, **6**, 1777–1813, 2006.

Tegen, I., Modeling the mineral dust aerosol cycle in the climate system, *Quaternary Science Reviews,* **22**, 1821–1834, doi:10.1016/S0277-3791(03)00163, 2003.

Untch, A., M. Miller, M. Hortal, R. Buizza, and P. Janssen, Towards a global meso-scale model: The high-resolution system T799L91 and T399L62 EPS, *ECMWF Newsletter*, No. 108, Summer 2006, 2006.

Wernli, H. and H. C. Davies, A Lagrangian-based analysis of extratropical cyclones. I: The method and some applications. Quart. J. Roy. Meteor. Soc., 123, 467-489, 1997.

Wu, L., Impact of Saharan air layer on hurricane peak intensity, *Geophys. Res. Lett.*, **34**, L09802, doi:10.1029/2007GL029564, 2007.

Development of spatially disaggregated on-road transport emission inventories for the Metropolitan Area of Buenos Aires, Argentina

Contributed by **Ariela D'Angiola**[1,3] (dangiola@cnea.gov.ar), **Laura Dawidowski**[2,4] *and* **Darío Gómez**[2,3,4]

[1]*Inter American Institute for Global Change Research –SAEMC Project*

[2]*Environmental Monitoring Group, Atomic Energy Commission of Argentina*

[3]*General San Martín National University*

Abstract

Emission inventories are essential for studies of both air quality and climate. The incorporation of local knowledge and locally specific emission factors and activity data are essential to building accurate local and global inventories for both of these types of studies. Here, a travel-based bottom-up approach was employed for the computation of annual emission inventories of criteria pollutants and greenhouse gases from on-road mobile sources for the year 2006 for the metropolitan area of Buenos Aires, Argentina. This was done for a range of spatial resolutions, making it useful for both local (e.g. air quality) and regional to global (e.g. climate) studies. Local, regional and international databases and methodologies were analyzed for the selection of the most representative emission factors for the 35 vehicle categories that make up the local fleet. A disaggregation methodology of the number of vehicles by district employing a socioeconomic parameter is hereby presented.

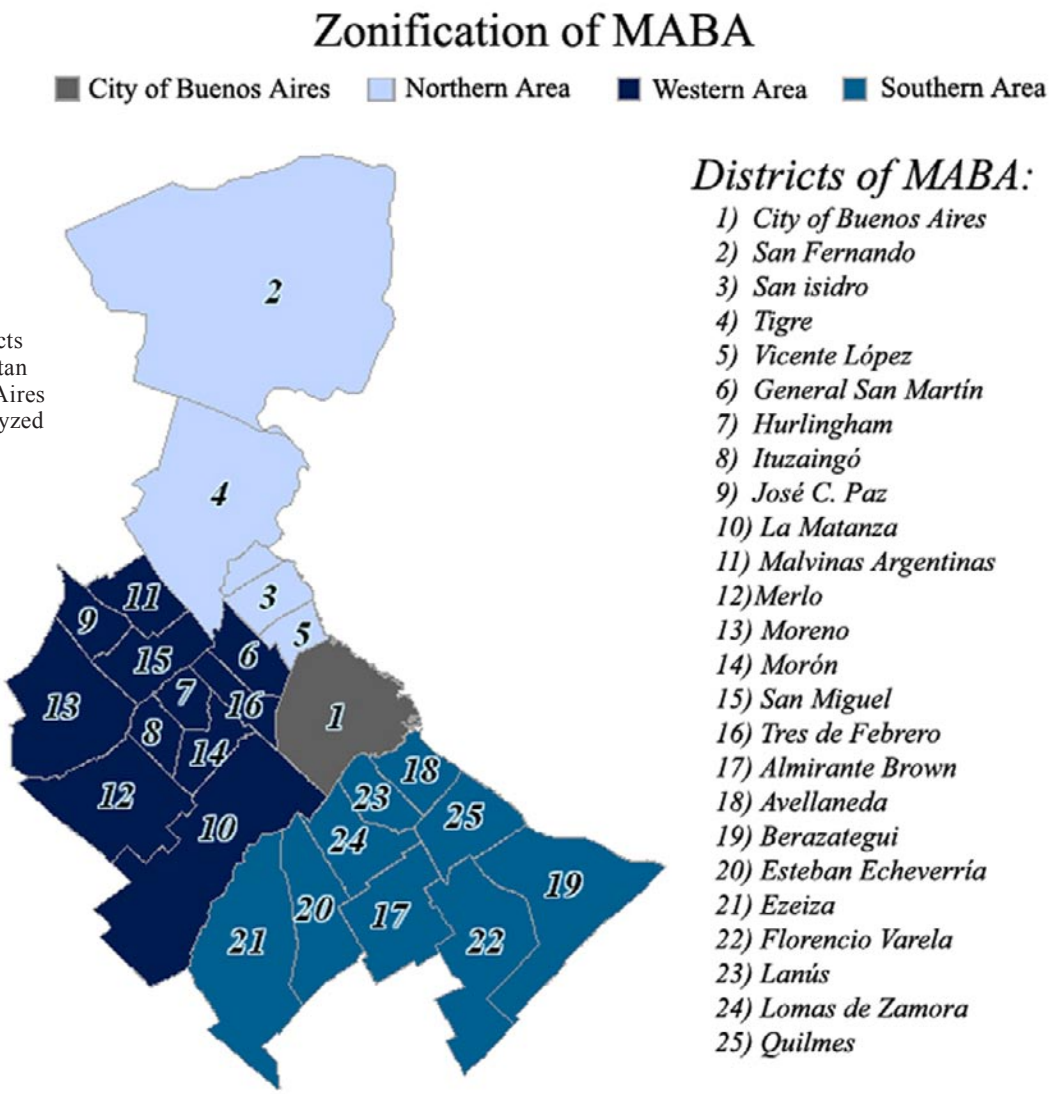

Figure. 1. Districts of the metropolitan area of Buenos Aires grouped by analyzed zone.

Table 1. Population data and number of registered vehicles by district and analyzed zone of the Metropolitan Area of Buenos Aires

ID	Metropolitan Area of Buenos Aires (Districts)	Population (Census 2001)	Projected Population (2006)	Area (km2)	Population Density (2006) (persons/ km2)	Registered Vehicles (PCs-SUVs-LDTs) (2006)	Nº of vehicles per capita (2006)	Population with UBN (%) (2001)
CBA	City of Buenos Aires	2,776,138	3,025,772	202.9	14,910	964,473	0.3188	7.8
SF	San Fernando	151,131	160,069	924	173	29,314	0.1831	16.1
SI	San Isidro	291,505	306,695	48	6,389	92,759	0.3024	8.3
TI	Tigre	301,223	328,760	360	913	51,639	0.1571	20.3
VL	Vicente López	274,082	285,121	39	7,311	85,118	0.2985	4.8
GSMA	General San Martín	403,107	421,419	56	7,525	80,092	0.1901	13.0
HU	Hurlingham	172,245	176,144	36	4,893	14,769	0.0838	12.6
IT	Ituzaingó	158,121	165,569	39	4,245	28,975	0.1750	10.8
JCP	José C. Paz	230,208	250,941	50	5,019	24,150	0.0962	26.7
LMA	La Matanza	1,255,288	1,338,386	323	4,144	161,946	0.1210	20.0
LZ	Lomas de Zamora	591,345	616,921	89	6,932	97,119	0.1574	17.2
MAL	Malvinas Argentinas	290,691	315,675	63	5,011	32,331	0.1024	22.9
ME	Merlo	469,985	512,875	170	3,017	52,061	0.1015	23.4
MOR	Moreno	380,503	426,065	180	2,367	39,063	0.0917	26.0
MON	Morón	309,380	328,301	56	5,863	94,640	0.2883	7.7
SMI	San Miguel	253,086	273,255	80	3,416	39,697	0.1453	18.2
TF	Tres de Febrero	336,467	345,880	46	7,519	69,710	0.2015	8.7
AB	Almirante Brown	515,556	555,589	122	4,554	64,150	0.1155	19.3
AV	Avellaneda	328,980	342,859	55	6,234	66,372	0.1936	10.7
BE	Berazategui	287,913	311,288	188	1,656	42,511	0.1366t	19.4
EE	Esteban Echeverría	243,974	264,072	120	2,201	34,292	0.1299	20.4
EZ	Ezeiza	118,807	136,124	223	610	12,306	0.0904	26.1
FV	Florencio Varela	348,970	390,163	190	2,053	32,788	0.0840	30.4
LAN	Lanús	453,082	463,564	45	10,301	90,026	0.1942	11.7
QU	Quilmes	518,788	541,972	125	4,336	87,772	0.1619	17.6
TOTAL		**11,460,575**	**12,283,479**	**3,830**		**2,388,071**		

Introduction

The Metropolitan Area of Buenos Aires (MABA) is the 10th largest megacity in the world and the 3rd largest in Latin America, with 12.8 million inhabitants (*UN, 2008*), accounting for 31% of the country's population but only 0.14% of the national territory. It comprises an area of 3,647 km^2 that extends 110 km N-S and 70 km E-W. It presents an average population density of 4,600 inhabitants per square kilometer and 2.4 million circulating vehicles distributed as follows: 93% passenger vehicles, 5% light-duty trucks and 2% heavy-duty trucks and buses. (See Table 1 for population data of the MABA). Following the geopolitical division proposed by the National Institute of Statistics and Census (*INDEC, 2001*), the MABA is composed of the City of Buenos Aires (the federal district that acts as the capital of the country) and the 24 radial surrounding districts that are part of the province of Buenos Aires (Figure 1).

According to the Greenhouse Gas National Emission Inventory of Argentina for the year 2000, on-road transport represents 30% of total CO_2 emissions and 55%

of total CO emissions, accounting for land use, land use change and forestry (*Fundación Bariloche, 2005*). As in many developing countries, despite the size of this highly populated urban zone, information on air quality is fragmentary and scarce, the availability of local and process-specific information on emissions represents a serious data gap (*Guttikunda et al., 2005*) and there is still no official inventory of mobile sources. The fact that three governmental levels (city, provincial and national) are present in the MABA has a direct effect on the availability, overlap and gaps in the consulted information sources. As a part of the South American Emissions, Megacities and Climate (SAEMC) 4-year regional project, the present emission inventories are being developed to provide input data for the modeling of regional air pollutant transport.

Methodology

The process of estimating mobile emissions is centered in a simple equation that combines *activity data* (number of vehicles and the kilometers traveled by them during the analyzed period of time) and an *emission factor* (which represents the emission rate per unit of activity that comes in the form of grams of pollutant emitted per kilometer traveled). Activity data can be determined through a range of procedures such as traffic surveys and transportation models, while emission factors are determined either under laboratory-controlled conditions for pre-determined driving cycles or using on-board emissions measurement instrumentation. Mobile source emission inventory calculations depend upon a large number of parameters: travel demand, traffic conditions, vehicle operating mode and conditions, type of vehicle, fuel characteristics, local climate conditions and topography (*Reynolds and Broderick, 2000*). For the present study, a bottom-up approach was implemented for the development of the emission inventories, therefore differences should be expected in comparisons to the national inventories. Here, the data employed is city-specific and is considered more accurate than national data, as the degree of detail is much higher since the geographical units covered are smaller (*Butler et al., 2008*).

Activity data (AD)

For the present fleet classification the considerations proposed in the COPERT[1] methodology (*Gkatzoflias et al., 2007*) were implemented, bearing in mind that despite the fact that the Argentinean fleet shares similarities with the European fleets, there exist important differences in the vintage of the average fleet and in vehicle maintenance practices. The local fleet was arranged in 35 categories divided by light-duty vehicles (passenger cars (PCs), sport utility vehicles (SUVs), taxicabs (TXs), light-duty trucks (LDTs)), and heavy-duty vehicles (heavy-duty trucks (HDTs), buses (Bs) and coaches (Cs)). These were further categorized according to fuel used and the implementation of emission control technology. The present categorization entails more accurate estimations of the emissions since each category has its own emission factor which is directly linked to age and technology parameters (*Zachariadis and Samaras, 2001*).

Different sources of information were considered for the activity data: the National Vehicle Registration Directory (DNRPA being its Spanish acronym), the Gas Regulatory Board of Argentina (ENARGAS), the Automobile Manufacturers Association (ADEFA), the Transport Regulatory Commission of Argentina (CNRT), and the Government of the City of Buenos Aires (GCBA). The total number of circulating PCs and SUVs registered in each district of the MABA until 2006 was provided by DNRPA for different time periods accounting for the implementation of the National Act 24,449 and particularly its resolution 779 in 1995 which established a two step process in the introduction of three-way catalyst (TWC) control (*DNRPA, 2007*). However, control and maintenance programs have not been thus far enforced, so for the purpose of these inventories it was assumed that vehicles registered before the year 2000 that were originally provided with a TWC do not posses such device in 2006 since TWCs have a lifetime of 5 years. Vehicles registered after year 2000 are considered to be equivalent to European vehicles following the EURO I emission standards and those registered after 2003, to EURO II. Information regarding trucks, buses and coaches was obtained from the annual bulletins reported by the CNRT (*CNRT, 2006*). The total number of LDTs and HDTs by district for the year 2005 was obtained from a study performed by the National Technological University (*C3T, 2007*). Following experts' recommendations HDTs were disaggregated into two categories, thus allowing for inclusion of emissions control technologies. Buses and coaches were all considered to be equivalent to European buses following the EURO II emission standards (*CNRT, 2006*). The number of taxicabs traveling in the City of Buenos Aires was provided by the GCBA, disaggregated by fuel type (*GCBA, 2005*). This information was not available for the surrounding districts of the MABA, for which taxicabs were considered in the inventories as PCs. Two-wheelers were not included because the corresponding activity data was not available. The DNRPA has only recently started to analyze and organize this information, which will be incorporated in future studies. For the present study, no scrappage methodologies were applied to the computed fleet because the consulted sources provided information on circulating vehicles for the year 2006, having dismissed old and invalid data.

The fuels employed in Argentina for on-road transport are gasoline, diesel oil and compressed natural gas (CNG). Unleaded gasoline has been mainly used by light-duty vehicles since 1998 when leaded gasoline was banned from the Argentinean market. Diesel oil has always been the fuel used by heavy-duty vehicles and is also employed by light-duty vehicles. The gasoline-diesel oil distribution for PCs, SUVs and LDTs categories was adopted from the DNRPA registries by district. CNG has become increasingly used in Argentina since 1995, especially due to its low market cost. Between 1995 and December 2006, 1.4 million vehicles in Argentina were

[1]COPERT III is a software program developed by the European Environment Agency as a European tool for the calculation of emissions from the road transport sector for the compilation of CORINAIR emission inventories.

Table 2. Distribution by vehicle category of the local fleet and corresponding vehicle kilometers travelled (VKT).

ID	Vehicle Type	Fuel	Emissions Control	Period of Registration	VKT	Fleet (2006)	Classification Characteristics
PC1	Passenger Cars	gasoline	No	<=1996	7,000	913,768	Vehicles of less than 2.5 tonnes with an engine size of 1.4-2.0 liters that are employed by private owners for their own travel needs.
PC2	Passenger Cars	gasoline	No	1997-2000	7,700	272,247	
PC3	Passenger Cars	gasoline	Yes	2001-2003	8,470	222,503	
PC4	Passenger Cars	gasoline	Yes	2004-2006	9,300	62,244	
PC5	Passenger Cars	diesel	No	<=2000	20,000	170,826	
PC6	Passenger Cars	diesel	Yes	2001-2003	22,000	81,822	
PC7	Passenger Cars	diesel	Yes	2004-2006	24,200	10,695	
PC8	Passenger Cars	CNG	No	<=2000	29,000	158,141	
PC9	Passenger Cars	CNG	Yes	2001-2006	31,900	115,187	
TX1	Taxicabs	diesel	No	<=2000	60,000	19,648	Vehicles of less than 2.5 tonnes with an engine size of 1.4-2.0 liters that are employed for passengers public transport; must be differentiated from PCs as they meet different travel demands (higher VKT).
TX2	Taxicabs	diesel	Yes	2001-2003	60,000	6,534	
TX3	Taxicabs	diesel	Yes	2004-2006	60,000	1,586	
TX4	Taxicabs	CNG	No	<=2000	60,000	5,071	
TX5	Taxicabs	CNG	Yes	2001-2006	60,000	5,559	
SUV1	Sport Utility Vehicles	gasoline	No	<=1996	7,000	56,542	Vehicles of less than 2.5 tonnes with an engine size > 2.0 liters that are employed by private owners for their own travel needs.
SUV2	Sport Utility Vehicles	gasoline	No	1997-2000	7,700	15,162	
SUV3	Sport Utility Vehicles	gasoline	Yes	2001-2003	8,470	12,204	
SUV4	Sport Utility Vehicles	gasoline	Yes	2004-2006	9,300	544	
SUV5	Sport Utility Vehicles	diesel	No	<=2000	20,000	85,517	
SUV6	Sport Utility Vehicles	diesel	Yes	2001-2003	22,000	22,647	
SUV7	Sport Utility Vehicles	diesel	Yes	2004-2006	24,200	795	
SUV8	Sport Utility Vehicles	CNG	No	<=2000	29,000	20,363	
SUV9	Sport Utility Vehicles	CNG	Yes	2001-2006	31,900	11,698	
LDT1	Light-Duty Trucks	gasoline	No	<=2000	18,000	31,603	Vehicles of less than 3.5 tonnes with an engine size < 2.0 liters that are employed for the local transport of goods; must be differentiated from SUVs as they meet different travel demands (higher VKT).
LDT2	Light-Duty Trucks	gasoline	Yes	2001-2003	19,800	4,545	
LDT3	Light-Duty Trucks	gasoline	Yes	2004-2006	21,780	357	
LDT4	Light-Duty Trucks	diesel	No	<=2000	55,000	42,471	
LDT5	Light-Duty Trucks	diesel	Yes	2001-2003	60,500	20,292	
LDT6	Light-Duty Trucks	diesel	Yes	2004-2006	66,550	556	
LDT7	Light-Duty Trucks	CNG	No	<=2000	67,500	5,989	
LDT8	Light-Duty Trucks	CNG	Yes	2001-2006	74,250	10,952	
HDT1	Heavy-Duty Trucks	diesel	No	<=2000	75,000	24,486	Vehicles of weight >3.5 tonnes that travel long distances for the transport of goods at provincial, national or international levels.
HDT2	Heavy-Duty Trucks	diesel	Yes	2001-2006	82,500	5,798	
B	Buses	diesel	Yes	<=2006	80,000	9,654	Urban public buses that travel around the MABA
C	Coaches	diesel	Yes	<=2006	13,500	10,560	Interurban buses that travel throughout the national territory
						2,438,569	

VKT = Vehicle kilometers traveled CNG= Compressed Natural Gas

retrofitted from gasoline to CNG, with 330,000 of these within the MABA region. The retrofitting process was more prevalent in commercial vehicles. CNG retrofitted vehicles are registered by vehicle type by ENARGAS.

Vehicle mileage is often collected by means of travel surveys, traffic counts and questionnaires to drivers. For this study, the total amount of fuel sold – gasoline, diesel oil and CNG – in 2006 in both geopolitical regions was considered to equal the amount that was actually consumed, and vehicle-kilometer statistics were combined with energy statistics by vehicle category and iteratively adjusted with fuel balance as closure. In order to obtain the representative vehicle-kilometers traveled (VKT) for MABA, whose districts share similarities between the City's and the Province's consumption patterns, the results were weighed with the registered fleet in each area. In addition, an age-dependent annual mileage was assumed, employing different mileage estimates for each model year group, since older vehicles tend to be driven less than new ones (*Zachariadis and Samaras, 2001*).

The final fleet classification with the corresponding vehicle kilometers travelled (VKT) is presented in Table 2.

Emission factors (EFs)

Following the 2006 IPCC Guidelines (*Goodwin et al., 2006*), local measurements of emission factors were complemented with regional and international databases in order to obtain a representative value for each compound and each category that would better characterize the local fleet. For this study emission inventories of carbon dioxide (CO_2), methane (CH_4), nitrous oxide (N_2O), carbon monoxide (CO), nitrogen oxides (NO_X), volatile organic compounds (VOCs), non-methane volatile organic compounds (NMVOCs), particulate matter (PM) and sulphur dioxide (SO_2) were computed.

In Argentina two different measurement campaigns were performed, both in the City of Buenos Aires. The first campaign began in the year 2000, during which four gasoline/CNG hybrid vehicles – three passenger cars (PCs) and one light-duty truck (LDT) – were tested for two years combining different air/fuel mixing ratios, measuring the resulting CO, NO_X and VOCs emissions with a dynamometer following the US FTP cycle (*Vasallo, 2000*). The second study was performed by ARPEL (Regional Association of Oil and Natural Gas Companies in Latin America and the Caribbean), Repsol YPF, Exxon Mobil and the GCBA in November 2004 on 25 running vehicles: 20 PCs and 5 LDTs that use gasoline, diesel oil and CNG as their only fuel or which were dually fuelled (gasoline and CNG). Here, CO_2, CO, NO_X and VOCs emissions were measured (*Acosta et al., 2006*).

As the available information is not enough to provide a robust set of local emission factors, information from a cluster of Latin American cities was assessed, taking into account driving conditions and fleet characteristics

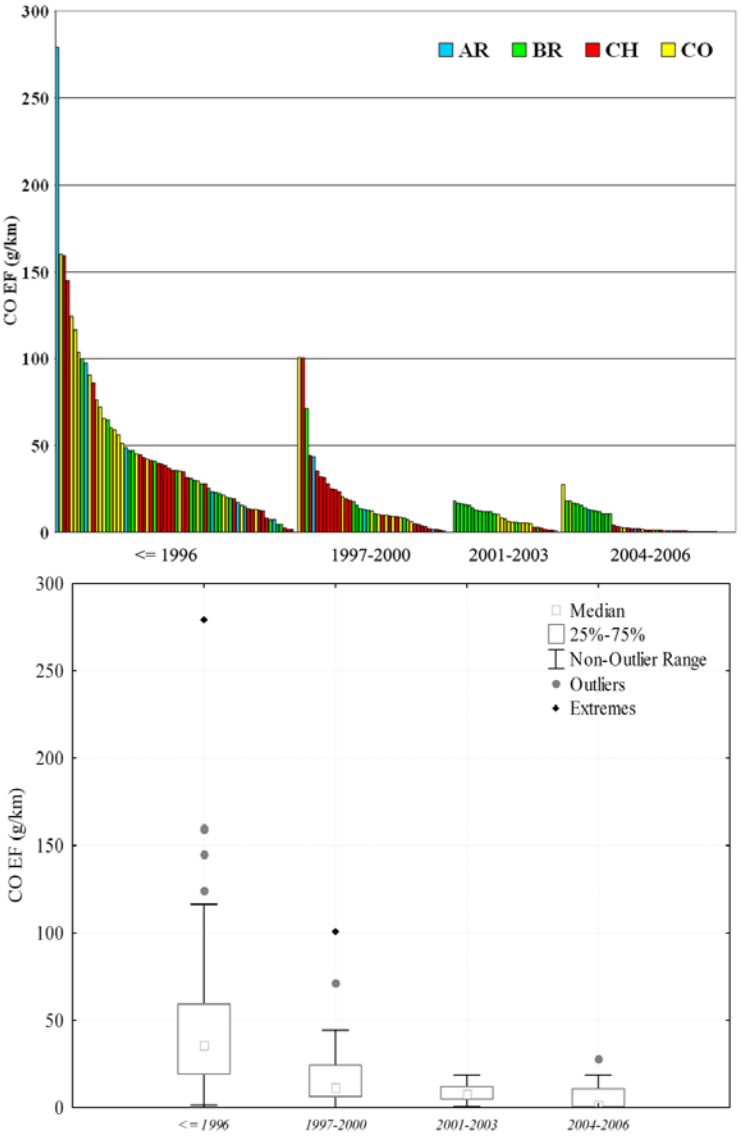

Figure 2. a) CO emission factors measured in Argentina (AR), Brazil (BR), Chile (CH) and Colombia (CO) for gasoline passenger cars according to year of registration; b) Distribution of the measured EF data for the 4 gasoline passenger cars´ categories and selected median values.

to identify a set of regional EFs best suited to the Argentinean conditions. The cities considered include Sao Paulo (Brazil), Bogota (Colombia), Santiago de Chile (Chile) and Mexico City (Mexico). Amongst the consulted sources, five corresponded to Brazil (*Martins et al., 2006*; *Rideout et al., 2005*; *Lents et al., 2007*; *CETESB, 2002-2007*; *MST, 2002*), two to Colombia (*Manzi et al., 2003*; *Behrentz and Rodriguez Vargas, 2008*), four to Chile (*Rideout et al., 2005*; *SECTRA, 2007*; *CONAMA-RM, 2008*; *Corvalan and Urrutia, 2000*) and one to Mexico (*Lents et al., 2007*).

The best-fitting distribution of each EF was assessed by means of Probability-Probability (P-P) Plots[2]. All data sets were adequately fitted by right-skewed distributions, which however did not follow a log-normal distribution (Figure 2a). Median values were selected since they are

[2]STATISTICA software (StatSoft Inc.)

Table 3. Final emissions factors by vehicle category (g km^{-1})

ID	VKT	CO_2	CH_4	N_2O	CO	VOCs	NMVOCs	NO_X	PM	SO_2
PC1	7,000	299	0.184	0.013	53.5	5.05	4.87	1.4	0.003	0.1136
PC2	7,700	299	0.184	0.013	17.2	1.97	1.78	0.9	0.003	0.1136
PC3	8,470	213	0.038	0.032	20.5	1.59	1.55	1.2	0.003	0.0810
PC4	9,300	213	0.043	0.017	2.6	0.26	0.21	0.2	0.003	0.0810
PC5	20,000	213	0.034	0.000	0.8	0.22	0.18	0.6	0.285	0.2016
PC6	22,000	182	0.016	0.002	0.5	0.08	0.06	0.7	0.078	0.1720
PC7	24,200	182	0.009	0.005	0.5	0.05	0.04	0.7	0.065	0.1720
PC8	29,000	239	0.709	0.068	6.4	2.27	1.56	1.7	0.000	0.0002
PC9	31,900	170	0.709	0.068	6.4	2.27	1.56	1.7	0.000	0.0001
TX1	60,000	213	0.033	0.000	0.8	0.22	0.19	0.6	0.285	0.2016
TX2	60,000	182	0.015	0.002	0.5	0.08	0.06	0.7	0.078	0.1720
TX3	60,000	182	0.008	0.004	0.5	0.05	0.04	0.7	0.065	0.1720
TX4	60,000	239	0.709	0.068	6.4	2.27	1.56	1.7	0.000	0.0002
TX5	60,000	170	0.709	0.068	6.4	2.27	1.56	1.7	0.000	0.0001
SUV1	7,000	366	0.184	0.013	81.5	8.93	8.74	2.6	0.003	0.1392
SUV2	7,700	366	0.184	0.013	14.8	1.97	1.79	1.0	0.003	0.1392
SUV3	8,470	286	0.038	0.032	15.4	1.10	1.06	0.9	0.003	0.1085
SUV4	9,300	285	0.043	0.017	7.4	0.48	0.44	0.5	0.003	0.1082
SUV5	20,000	213	0.034	0.000	0.8	0.22	0.18	0.9	0.285	0.2016
SUV6	22,000	234	0.016	0.002	0.5	0.12	0.10	0.7	0.078	0.2209
SUV7	24,200	234	0.009	0.005	0.5	0.14	0.14	0.7	0.065	0.2209
SUV8	29,000	292	0.709	0.068	10.8	2.27	1.56	2.5	0.000	0.0002
SUV9	31,900	228	0.709	0.068	10.8	2.27	1.56	2.5	0.000	0.0002
LDT1	18,000	365	0.184	0.013	33.3	4.56	4.38	1.2	0.003	0.1387
LDT2	19,800	365	0.038	0.044	26.4	3.11	3.07	1.6	0.003	0.1387
LDT3	21,780	365	0.043	0.036	22.5	2.23	2.19	1.5	0.003	0.1387
LDT4	55,000	279	0.034	0.000	1.4	0.18	0.15	2.1	0.367	0.2638
LDT5	60,500	252	0.016	0.002	0.5	0.18	0.17	1.3	0.100	0.2378
LDT6	66,550	252	0.009	0.005	0.5	0.18	0.17	1.3	0.100	0.2378
LDT7	67,500	291	0.709	0.068	1.6	0.80	0.09	1.9	0.000	0.0002
LDT8	74,250	291	0.709	0.068	1.6	0.80	0.09	1.9	0.000	0.0002
HDT1	75,000	837	0.171	0.029	3.9	3.69	3.52	8.9	1.054	0.7906
HDT2	82,500	837	0.171	0.011	1.8	0.69	0.52	5.6	0.170	0.7906
B	80,000	771	0.111	0.012	6.1	1.43	1.32	16.0	0.190	0.7283
C	13,500	893	0.111	0.011	6.1	1.43	1.32	16.0	0.190	0.8437

a better indication of the central tendency of the data. As a subsequent step of this research, lower and upper quartile values will be employed as a measure of uncertainty contributions to the inventories, bearing in mind that emissions estimates obtained by the application of such emission factors are associated with significant uncertainty due to the highly scattered experimental data. For example, the distribution of the CO emission factors for the four technology categories in the box and whiskers plot in Figure 2b indicate its high dispersion and skewness. The final incorporation of the computed EFs depended on the sample size of each data set, with a required minimum of 30 measurements for light-duty vehicles and 15 for heavy-duty vehicles (*CONAMA-RM, 2008*). All gasoline vehicles (PCs, SUVs, and LDTs) and diesel-fuelled Bs, Cs and HDTs had enough values for all the analyzed species in order to include the median EFs to the

inventories' computation, excepting CH_4 and N_2O. With regards to CNG vehicles, emission factors for CO_2, CO, NO_X, and VOCs were obtained from these analyses.

Taking into consideration the similarities between Latin American and European fleets proposed by Economopoulus (*1993*) and the fact that European models comprise a large fraction of the Argentinean fleet, the algorithms of the COPERT methodology (*Gkatzoflias et al., 2007*) were incorporated into the analysis. This methodology allows computation of emission factors for different vehicle categories which reflect legislative and technological steps (i.e. incorporation of emission control devices as well as emission reductions). The algorithms for the computation of emission factors for the following categories were incorporated to the inventories' computation from the COPERT 4 model: a) emission factors for all species for diesel light-duty vehicles (PCs, SUVs, and LDTs), because for these categories there were fewer than the minimum requirement for 30 samples; b) CH_4 and N_2O emission factors for all gasoline and diesel-fuelled vehicle categories, as there is almost no measured data for these compounds; and c) available cold-start emission factors were calculated for all vehicle categories and for all species, as the measured values were all obtained from vehicles operating with hot engines. For all vehicle categories, an urban average speed of 35 km h^{-1} was employed as given by a study performed in the MABA (*Acosta et al., 2006*). We note that the emission factors proposed by MOBILE 6 (*USEPA, 2003*) were discarded due to its highly demanding data input. Emissions factors proposed by the IPCC (*EFDB*) for CH_4 and N_2O for CNG vehicles were incorporated into the computations, as they represent the only source of information for these species for the named categories.

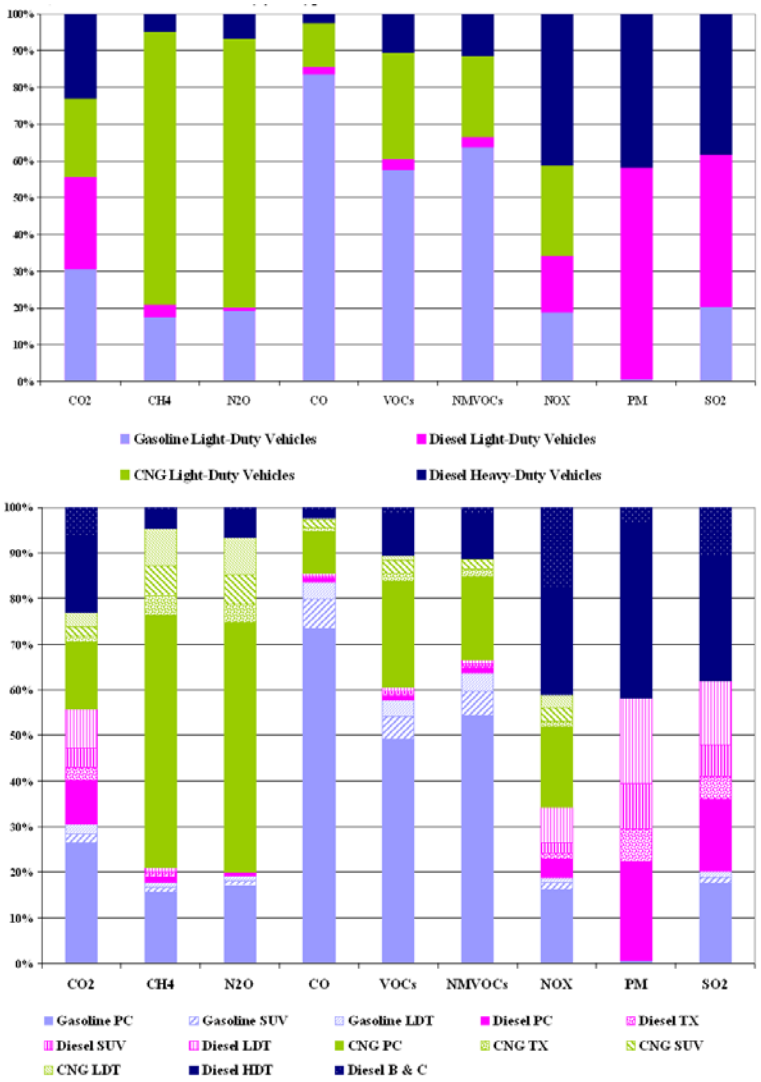

Figure 3. a) Emissions distribution by fuel type; b) Emissions distribution by vehicle category

The resulting emissions factors, by species and vehicle category, are presented in Table 3.

Results

Emission inventories

Annual emissions for the metropolitan area of Buenos Aires for the year 2006 from the on-road mobile sector are given in Table 4. Figure 3a presents the distribution of emissions according to vehicle type (light-duty vehicles grouped according to fuel used and diesel heavy-duty vehicles), showing the contribution of each to the emissions of the different species. These are computed directly from the fuel consumption within each category, and it is interesting to note that the four main groups were almost equally responsible for CO_2 emissions. In spite of the fact that heavy duty vehicles were small in number compared to the total fleet, their CO_2 emissions almost equaled those of gasoline and diesel vehicles because of their high number of vehicle kilometers traveled and their high fuel consumption values. Gasoline Light-Duty vehicles were the main emitters of CO and VOCs, accounting for almost 85% of CO emissions and 60% of VOCs emissions, while they only represented a small fraction (20%) of CH_4, N_2O, NO_X and SO_2 emissions. On the other hand, Diesel Light and Heavy-Duty vehicles together were responsible for almost all PM emissions, 70% of SO_2 emissions and 55% of NO_X emissions, while they accounted for only 4% of CO emissions. CNG Light-Duty vehicles represented 70% of CH_4 and N_2O emissions.

These emissions were further disaggregated by more specific vehicle categories, showing the importance of understanding these specific categories' contributions in the computation of the final emissions (Figure 3b). Gasoline passenger cars registered before 1997 were the highest emitters of CO, VOCs, NMVOCs and CO_2, accounting for 60%, 40%, 45% and 17% of total emissions respectively. This category was composed of old vehicles with no emissions control devices nor maintenance, making them very difficult to characterize with a single emission factor. The inclusion of regional

emission factors was crucial for this category in particular as emission factors measured in developed countries do not properly characterize the emissions from these old vehicles, thus highlighting the importance of obtaining local measurements. Emission factors for Diesel Heavy-Duty Trucks were generated using data on number of vehicles and vehicle kilometers travelled that are highly uncertain. This had the largest effect on the partitioning of emissions of CO_2, NO_X, PM and SO_2, where HDTs are responsible for 17%, 23%, 39% and 28% of emissions respectively.

These results demonstrate the importance of improving knowledge of vehicle number, the technology distribution of all vehicle types, and having more emission factors measurement campaigns with local vehicles operating on local driving cycles.

Reconstruction of Activity Data

Since in most developing countries activity data is not readily available, especially in provinces or districts outside the capital cities, a number of socioeconomic variables from the national census (*INDEC, 2001*) and the United Nations Development Program (UNDP) were explored in order to identify the parameter that would best infer the number of vehicles registered in each district. Total population, population density, number of

Table 4. Emissions (Gg year-1) for the year 2006 by district of the Metropolitan Area of Buenos Aires

District	CO_2	CH_4	N_2O	CO	VOCs	NMVOCs	NO_X	PM	SO_2
AB	257	0.27	0.025	16.2	2.1	1.8	1.7	0.09	0.12
AV	278	0.29	0.027	16.5	2.1	1.8	2.0	0.09	0.14
BE	168	0.18	0.017	10.7	1.4	1.2	1.0	0.06	0.08
CBA	4,751	4.26	0.431	211.1	30.9	26.6	31.4	2.20	2.80
EE	139	0.15	0.014	8.6	1.1	1.0	0.9	0.05	0.07
EZ	47	0.05	0.005	3.1	0.4	0.3	0.3	0.02	0.02
FV	131	0.14	0.013	8.5	1.1	0.9	0.8	0.05	0.06
GSMA	320	0.35	0.032	20.5	2.6	2.3	2.1	0.10	0.15
HU	63	0.06	0.006	3.7	0.5	0.4	0.5	0.02	0.03
IT	117	0.12	0.012	7.1	0.9	0.8	0.8	0.04	0.06
JCP	96	0.10	0.009	6.4	0.8	0.7	0.6	0.03	0.05
LMA	671	0.70	0.065	40.5	5.2	4.5	4.5	0.24	0.33
LAN	384	0.39	0.037	22.2	2.9	2.5	2.7	0.14	0.20
LZ	406	0.42	0.039	23.9	3.1	2.7	2.9	0.14	0.20
MAL	130	0.14	0.013	8.5	1.1	0.9	0.9	0.04	0.06
ME	206	0.22	0.020	13.7	1.7	1.5	1.4	0.07	0.10
MOR	161	0.17	0.016	10.1	1.3	1.1	1.1	0.06	0.08
MON	385	0.41	0.038	23.3	3.0	2.6	2.7	0.13	0.19
QU	358	0.38	0.035	20.9	2.7	2.3	2.3	0.13	0.18
SF	111	0.12	0.012	7.2	0.9	0.8	0.7	0.03	0.05
SI	342	0.39	0.038	21.1	2.8	2.4	2.2	0.10	0.16
SMI	158	0.17	0.016	9.9	1.3	1.1	1.1	0.05	0.08
TI	209	0.22	0.021	13.0	1.7	1.5	1.4	0.07	0.10
TF	300	0.30	0.028	17.6	2.3	2.0	2.2	0.10	0.15
VL	321	0.36	0.035	19.7	2.6	2.2	2.2	0.09	0.15
HDVs North	177	0.03	0.005	0.9	0.6	0.6	2.1	0.17	0.17
HDVs West	470	0.09	0.015	2.1	1.9	1.8	5.0	0.52	0.44
HDVs South	393	0.08	0.012	1.8	1.5	1.4	4.3	0.42	0.37
Total	**11,548**	**10.57**	**1.036**	**568.8**	**80.4**	**69.8**	**81.9**	**5.24**	**6.60**

HDVs= Heavy-Duty Vehicles (Trucks, Buses and Coaches)

vehicles, number of vehicles per capita, the percentage of the population with unsatisfied basic needs (UBN), GDP, and the human development index (HDI) of the UNDP were all analyzed. The UBN index, computed by the ECLAC (Economic Commission for Latin America and the Caribbean) indicates the percentage of the population with poor housing and crowding conditions, sanitation, school attendance, and subsistence capacity, computed with high level of spatial disaggregation. This appears to be the most appropriate factor for determining the number of vehicles per capita by district, as given by a correlation factor (r^2) of 0.91 (Figure 4).

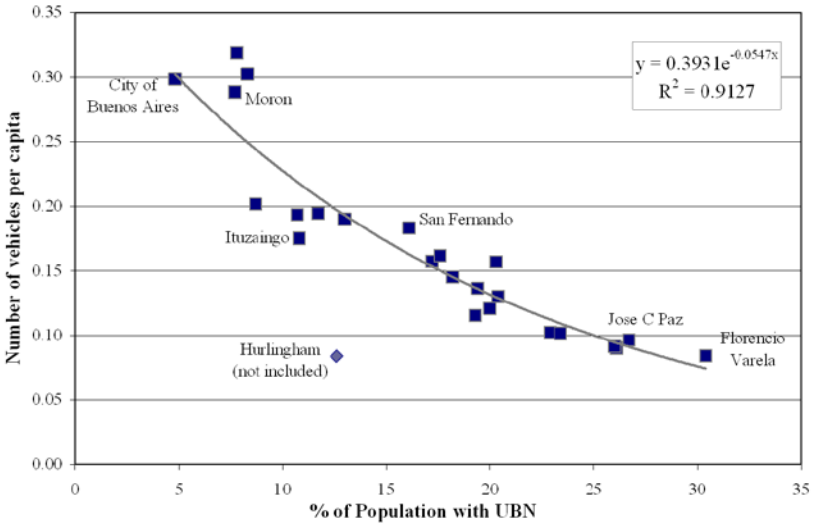

Figure 4. Correlation between the number of vehicles per capita and the UBN index for the districts of the MABA.

Emissions Disaggregation

a) By district

With the information provided by the DNRPA, emission inventories for each district were compiled employing only vehicles of private and commercial use that did not perform a controlled and specific route of transport: passenger cars, taxicabs, sport-utility vehicles and light-duty trucks. Figure 5 presents the spatial distribution of 2006 CO and PM emissions. Emissions of CO correlate with the registration of vehicles, accounting for their type and number, whereas PM emissions correlate with the number of registered diesel vehicles.

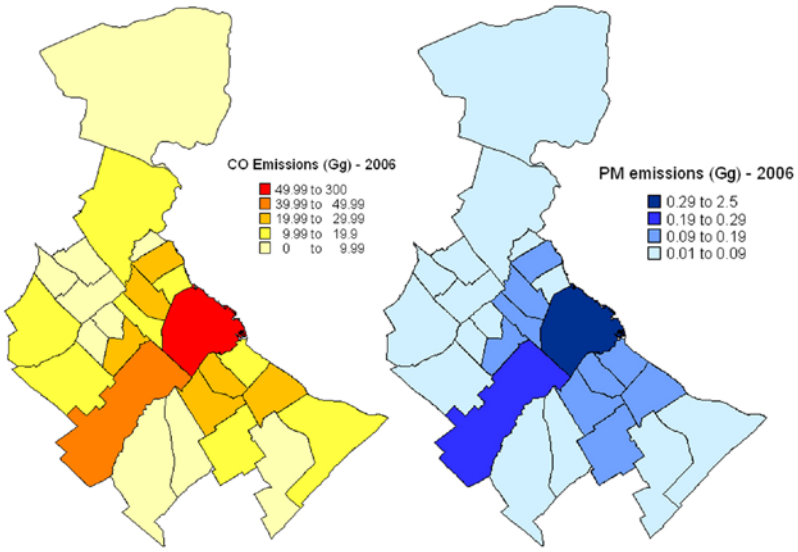

Figure 5. Spatial disaggregation of a) CO emissions (Gg year^{-1}) and b) PM emissions (Gg year^{-1}) by district

b) By street length

For regional and inverse modeling purposes, the computed emissions were disaggregated in a 1000 celled-grid of DX=DY=0.018°. Considering the characteristic routes and traffic patterns of the different types of vehicles, emissions were spatially distributed using the following assumptions to scale the emissions from each source:

- Light-Duty Vehicles: Emissions scaled with the inverse UBN index and the total length of streets within each cell. It was assumed that the circulation of these vehicles increased in high income areas.
- Heavy Duty Trucks and Coaches: Emissions scaled with the total street distance (length) of the Heavy-Duty transport network within each cell.
- Urban Buses: Emissions scaled with the UBN index and the total length of streets within each cell. It was assumed that the circulation of these vehicles increased in low income areas.

Total emissions were distributed in each cell using the compound factor λ_i:

$$m_{ij} = \lambda_i * M_j$$

$$\lambda_i := UBN_i * L_i / \Sigma (UBN_i * L_i)$$

where:

m_{ij}= emissions of species j in cell i,

M_j= total emissions of species j

UBN_i = Unsatisfied Basic Needs index for cell i

L_i = Length of Streets within cell i

Spatial disaggregation of CO emissions resulted mostly from Light-Duty vehicles (PCs, SUVs, and LDTs) that were registered in each district (Figure 6), thus following registration patterns. When analyzing other compounds, especially those such as PM which are related to heavy duty vehicles, the mapping of emission follows the driving patterns of these vehicles.

Conclusions

In this work, the results of 2006 annual emission inventories of CO_2, CH_4, N_2O, CO, NO_X, VOCs, NMVOCs, PM and SO_2 for the metropolitan area of Buenos Aires, Argentina, are reported, together with the variables that contribute to emissions, i.e.: number of vehicles, vehicle kilometers travelled and emission factors. An accurate representation of the local fleet was obtained through the collection of local data. Where local information was not available, data from a cluster of Latin American cities was selected to generate regional information that is most suitable to the local conditions of the Metropolitan Area of Buenos Aires.

The computed emissions were spatially disaggregated into a 1000 celled grid according to the total length of streets within each grid cell and the Unsatisfied Basic Need (UBN) index, to be employed for regional and inverse modeling purposes.

An innovative approach for the determination of the registered vehicles by district was developed, relating the socioeconomic parameter UNB index with the number of vehicles per capita, with a correlation coefficient of 0.91.

This research is still in progress and what remains to be tackled are the associated uncertainties.

Acknowledgments

This work was carried out with the aid of a grant from the Inter-American Institute for Global Change Research (IAI) CRN II 2017 which is supported by the US National Science Foundation (Grant GEO-0452325), and within the Project PICT 32494 funded by the Agencia Nacional de Promocion Cientifica y Tecnologica, Argentina.

References

Acosta A., Ferro R., Herrero Rosas M., Schreck B., Medición de emisiones vehiculares en la ciudad de Buenos Aires, Petrotecnia, 2006.

Behrentz E. and Rodriguez Vargas P.A., IVE campaign-phase II developed by CIIA (Environmental Engineering Research Center), University of Los Andes, Bogota, Colombia, personal communication, 2008.

Butler, T.M., Lawrence, M.G., Gurjar, B.R., Van Ardenne, J., Schultz, M., Lelieveld, *The representation of emissions from megacities in global emission inventories*, J. Atmospheric Environment 42, 703-719, 2008.

C3T, El Transporte Automotor de Cargas en la Argentina, Centro Tecnológico de Transporte, Transito y Seguridad Vial, Secretaria de Extensión Universitaria, Universidad Tecnológica Nacional, edUTecNe, 2007. Available at http://www.utn.edu.ar/secretarias/extension/c3tlibro.utn

CETESB, *Relatório de qualidade do ar no Estado de São Paulo 2001-2006*, Série Relatórios / Secretaria de Estado do Meio Ambiente, ISSN 0103-4103, São Paulo, 2002-2007.

CNRT, Cortes A. and Domecq R., personal Communications,

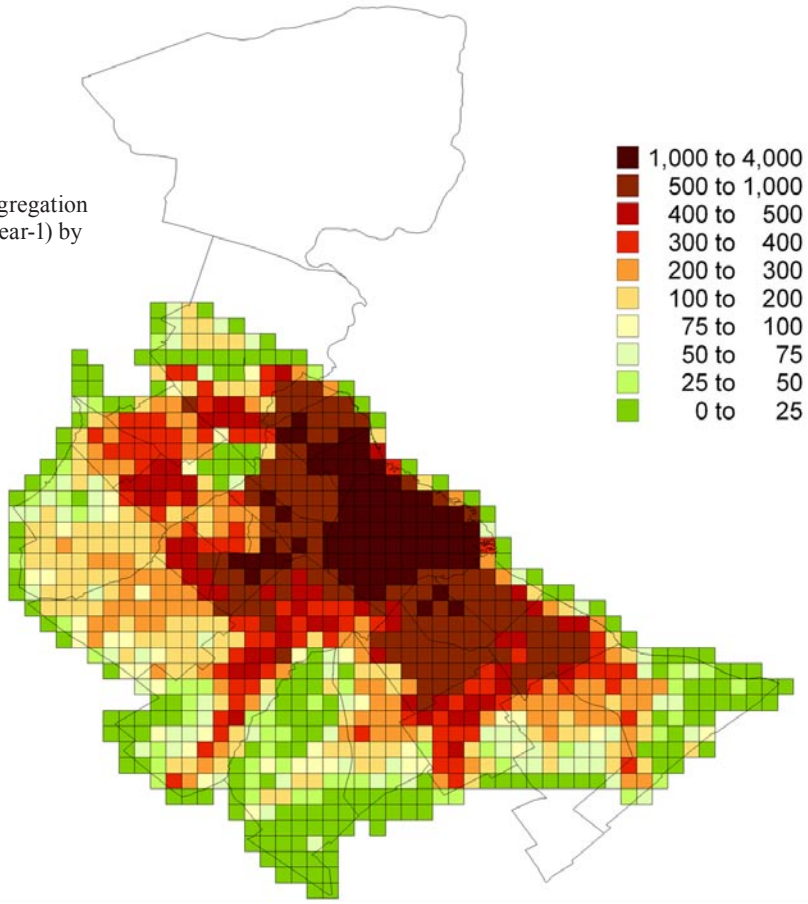

Figure 6. Spatial disaggregation of CO emissions (Gg year-1) by gridcell.

2006.
CONAMA-RM, *Generación de factores de emisión para vehículos livianos, medianos y pesados de la Región Metropolitana, Informe final*, Comisión Nacional del Medio Ambiente, Santiago de Chile, 2008.
Corvalan R.M. and Urrutia, C.M., *Emission Factors for Gasoline Light-Duty Vehicles: Experimental Program in Santiago-Chile*, Journal of the Air & Waste Management Association, vol. 50, nº 12, pages 2102-2111, 2000.
DNRPA, 2007, Alcaraz A.; Arcidiacono, S.; Guelfo, M.; Sadi J., personal communication, 2007.
Economopoulus A., *Assessment of sources of air, water, and land pollution: a guide to rapid source inventory techniques and their use in formulating environmental control strategies*, World Health Organization, 1993.
EFDB, *Emission Factors Database*, Intergovernmental Panel on Climate Change, National Greenhouse Gas Inventories Programme. <http://www.ipcc-nggip.iges.or.jp/EFDB/>
Fundación Bariloche, *Inventario Nacional de la República Argentina, de fuentes de emisiones y absorciones de gases de efecto invernadero, no controlados por el Protocolo de Montreal, Inventario correspondiente al año 2000 y revisión de los inventarios 1990, 1994 y 1997,* Buenos Aires, Argentina, 2005.
GCBA, Bormioli M., personal communication, 2005.
Gkatzoflias D. Kouridis C., Ntziachristos L. and Samaras Z., *COPERT 4 Computer Programme to Calculate Emissions from Road Transport, (Version 5.1)*, European Environmental Agency ETC/AEM, 2007. <http://lat.eng.auth.gr/copert/>
Goodwin J., Woodfield M., Ibnoaf M., Koch M. and Yan H., Approaches to Data Collection. Chapter 2, Volume 1, 2006 IPCC Guidelines, 2006.
Guttikunda, S. K., Y. Tang, G. R. Carmichael, G. Kurata, L. Pan, D. G. Streets, J.-H. Woo, N. Thongboonchoo, and A. Fried, *Impacts of Asian megacity emissions on regional air quality during spring 2001*, J. Geophys. Res., 110, D20301, doi:10.1029/2004JD004921, 2005.
INDEC, *Censo Nacional de Población, Hogares y Viviendas del año 2001*, Instituto Nacional de Estadística y Censos, Argentina, 2001. <http://www.indec.gov.ar/webcenso/index.asp>
Lents J., Nickila N., Davis N., Canada M., Martinez H., Osses M., Tolvett S., *A Study of the Emissions from Diesel Vehicles Operating in Sao Paulo, Brazil and in Mexico City, Mexico*, 2007.
Manzi V., Belalcazar L.C., Giraldo E., Zarate E. and Clappier A., *Estimación de los Factores de Emisión de las Fuentes Móviles de la Ciudad de Bogotá*, Revista de Ingenieria n° 18, Facultad de ingenieria, Universidad de los Andes, 2003.
Martins, L.D., Andrade M.F., Freitas E., Pretto A., Gatti L.V., Albuquerque E.L., Tomaz E., Guardani M.L., Martins M.H.R.B. and Junior O.M.A., *Emission Factors for Gas-Powered Vehicles Traveling Through Road Tunnels in Sao Paulo, Brazil*, Environmental Science & Technology, 40(21), 6722-6729, 2006.
MST, *First Brazilian Inventory Of Anthropogenic Greenhouse Gas Emissions, Reference Report Greenhouse Gas Emissions From Movable Sources In The Energy Secto*r, Ministry Of Science And Technology, 2002.
Reynolds A.W., Broderick B.M., *Development of an emission inventory model for mobile sources*, J.Transportation Research Part D 5, 77-101, 2000.
Rideout G., Gourley D., Walker J., *Measurement of In-Service Emissions in Sao Paulo, Santiago and Buenos Aires*, ARPEL Environmental Report # 25, 2005.
SECTRA, *Actualización de Factores de Emisión para Vehículos Livianos Y Medianos*, Secretaría Interministerial de Planificación de Transporte, Santiago de Chile, Chile, 2007.
SECTRA, *Investigación de Factores de Emisión para Vehículos de Carga*, Secretaría Interministerial de Planificación de Transporte, Santiago de Chile, Chile, 2007.
UN, *An Overview of Urbanization, Internal Migration, Population Distribution and Development in the World*, Population Division, Department of Economic and Social Affairs, United Nations Secretariat, New York, 2008.
USEPA, *User's Guide to MOBILE 6.1 and MOBILE 6.2 Mobile Spurce Emission Factor Model,* EPA420-R-03-010, Environmental Protection Agency, United States, 2003. <http://www.epa.gov/otaq/m6.htm>
Vasallo J.E., *Experiencia y Datos Técnicos del GNC en la Argentina*, presented at the XXVII Interamerican Conference on Environmental Sanitary Engineering, Porto Alegre, Brazil, 2000.
Zachariadis T., and Samaras Z., *Validation of road transport statistics through energy efficiency calculations*, Energy 26, 2001, 467-491, 2001.

Ice and halogens: laboratory studies to improve the modelling of field data

Contributed by **John Sodeau** *(j.sodeau@ucc.ie), University College Cork, Department of Chemistry and Environmental Research Institute, Cork, Ireland.*

Introduction

In the past 10 years or so there has been an explosion of interest, research, and reports regarding studies of chemical exchange between the atmosphere and the cryosphere, chemical processes mediated by ice and snow surfaces, and halogen chemistry in polar regions, both in the troposphere and stratosphere. A great deal of the work has been summarized in a recent, special issue of Atmospheric Chemistry and Physics, which is referenced below. However, while there has been a fantastic increase in our awareness of the importance of these processes to the ultimate composition of the atmosphere, our fundamental understanding of the driving chemical and physical process, and, as a consequence, our ability to simulate them using computer models, is severely limited at this time. We clearly need at this point to better connect the field research community with the communities studying relevant processes in the laboratory and those using models, as well as connect those working on these issues in the context of the polar lower troposphere and those focusing on heterogeneous and cold-temperature reactions in the stratosphere. Given recent advances in knowledge it is timely for these communities to explore and define (where there are suitable challenges and opportunities) the possibilities for new laboratory studies that will answer critical open questions. Hence members of two IGAC Tasks "Air Ice Chemical Interactions" (AICI; http://www.igac.noaa.gov/AICI.php & *IGACtivities* issue No. 29) and "Halogens in the Troposphere" (HitT; http://www.igac.noaa.gov/HitT.php & *IGACtivities* issue No. 39) as well as members of WCRP's Stratopsheric Processes and their Role in Climate project (SPARC; http://www.atmosp.physics.utoronto.ca/SPARC-IPY/) convened a workshop at the British Antarctic Survey (BAS) in June of 2008.

Two specific targets were set up in order to provide a Framework for the workshop discussions:

i. To address the questions which have arisen within both the recent Issue of Atmospheric Chemistry and Physics (Vol 7) published in 2006/2007 (http://www.atmos-chem-phys.net/special_issue80.html; see References below) and within the stratospheric community, via SPARC.

ii. To introduce this science to a new group of researchers both at Senior and PhD level, and in doing so to encourage collaboration across areas of expertise (i.e. field measurements, lab measurements and modeling).

The workshop program was divided into six half-day sessions, each with a "Discussion/Tutorial Leader":

1. Surface and Bulk Properties of Ices and Clouds
2. New Experimental Approaches to the Study of Ices and Aerosols
3. Halogen Activation in the Atmosphere
4. Mercury in the Cold
5. Kinetics of the Cold Atmosphere
6. Outcomes and Challenges

The Workshop was constructed to be deliberately laboratory-centric in nature but many participants with field and modeling interests also attended to provide an essential sense of atmospheric perspective. Over fifty scientists attended and from the feedback that the organizers received, many new ideas were stimulated and several new collaborations between laboratory, field and the "virtual" world were forged. A BAS-hosted web-site has been developed to archive the workshop presentations and discussions (for participant access). Here we summarize critical aspects of the discussions as well as the main conclusions and recommendations, as presented by Paul Shepson and Tony Cox in the final half-day session. In particular they addressed the future role of the AICI team so this specifically is discussed at the end of this article.

Scientific Topics

Each of the thematic half-day sessions was constructed to allow about two hours in total of discussion time with about four lectures presented. Only a flavor of the material presented can be shown in this article and so just four examples are given (see boxes) to highlight the breadth of studies currently being undertaken to help understand the atmospheric chemistry that occurs in the polar regions.

Workshop Summary: Outcomes and Challenges

Considerable progress has been made in the area of ice/atmosphere interactions in the context of atmospheric chemistry and composition in the polar regions. We know that there is an important role of heterogeneous reactions in controlling the main trace gases and more esoteric species like mercury; a knowledge of reactive halogen chemistry is central to this.

However we do not have enough quantitative information and understanding of basic parameters yet to formulate a predictive numerical model. This is particularly true of chemical processes occurring at the air/ice interface and the physical processes involved in production and loss of atmospheric particulate material. This leads to large uncertainties in the source terms for reactive gases (halogens, NO_x species, Hg, etc.) and quantification of the recycling of these gases in the

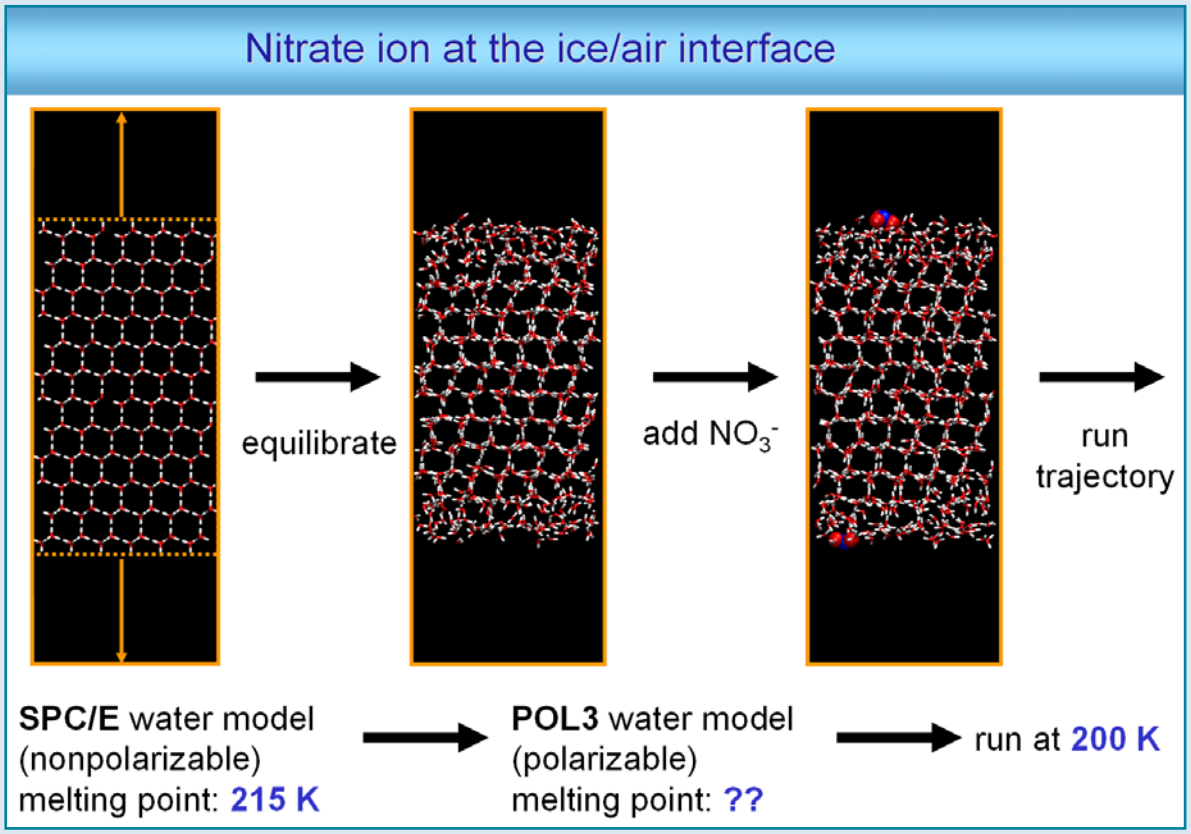

Molecular dynamics simulations are used to gain insight at a molecular level into the structure and dynamics of the ice/vapor interface. Of particular interest is the effect of ions on the properties of the interfacial region. Adequate modeling of the distribution of ions within the quasi-liquid/brine layer on the surface of ice is likely to require explicit treatment of polarization interaction. This figure schematically shows the simulation protocol employed in a preliminary study of a nitrate ion at the ice/vapor interface using a polarizable model. (*Courtesy of Martina Roeselova, Academy of Sciences of the Czech Republic, Prague, Czech Republic*)

polar environment.

Therefore one important role of the AICI and HitT Tasks has been to assist the community in leveraging and coordinating our combined intellectual and tangible assets, and documenting our priorities/needs in the area of atmospheric chemistry at the ice/atmosphere boundary. The BAS Workshop is one of the ways in which the community has attempted to do this and the following broad issues/questions arose:

- How can we best advance the field of research and its fundamental science?
- How can we coordinate/combine resources?
- What is the best way to influence international support for the studies?

The lectures and extensive discussions that took place in Cambridge expanding on these points can be divided into the following categories: 1. Technology Development; 2. Laboratory Studies; 3. Shared Facilities; 4. Coordinated/Scientifically Focused Field Studies; 5. Data Exchange, Evaluation and Assessment; 6. Modeling studies.

1. Technology Development

Much discussion centered on areas where new observation techniques were needed to answer fundamental questions relating to the physical and chemical processes around air-ice interactions. For example: How to best measure the density of "dangling OH" bonds: surface spectroscopy or chemical interrogation? What techniques can be employed to observe adsorbates on surfaces and to examine 3D chemical morphology and surface pH? What techniques might be developed to observe characteristics of the Quasi-Brine Layer (QBL) on real ice surfaces?

At a more fundamental level there was much discussion regarding the need to understand what the terms quasi-liquid layer (QLL) or quasi-brine layer (QBL) actually mean, in physical and chemical terms. Hence for laboratory studies, researchers need to know how to make a *relevant* phase/system in which to study kinetics and mechanisms. However little is known about the

Satellite observations show that blooms of Iodine Monoxide *(right)* (IO; i.e. see *Schönhardt, A. et al., 2008*) and of Chlorophyll-a *(below)* in the Antarctic sea ice zone are coincident. This confirms the first of a set of steps leading to the theory that diatoms emit iodine compounds which grow new particles, thereby allowing sea ice biota to affect regional climate in a way which implies positive feedback.

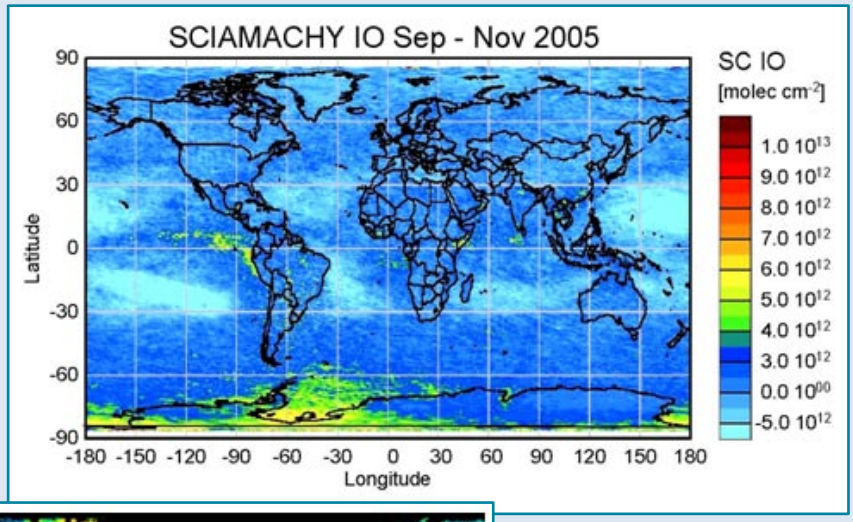

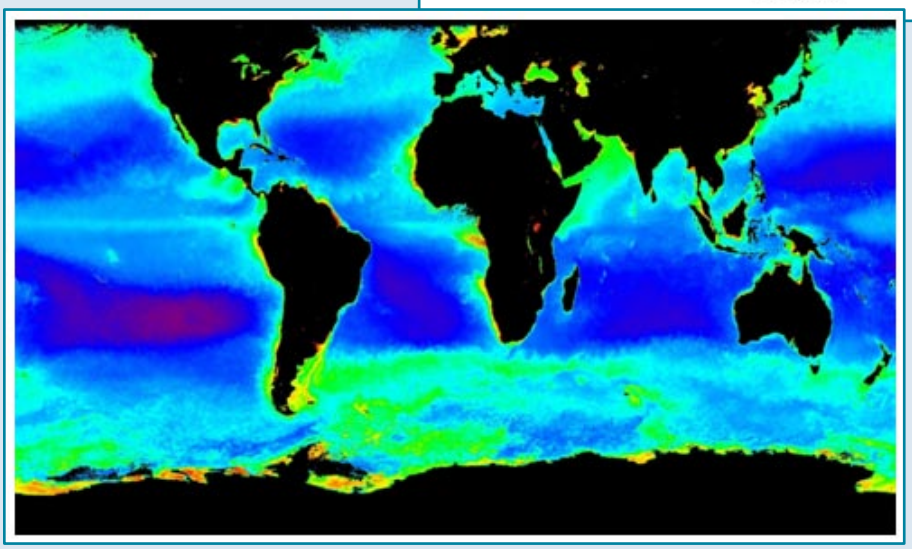

(*Courtesy Howard Roscoe, British Antarctic Survey, Cambridge, U.K.*)

composition of reactants in these environments. Tools that can distinguish between them are required along with methods to determine thickness and coverage.

It was also felt that techniques to provide speciation data and the quantification of a variety of relevant chemical systems are needed. In this regard a main issue continues to centre on the chemical nature of Reactive Gas-phase Mercury but there are also needs for determining other "exotic" but usefully-observed species, such as bromo-PAN. Finally many questions about the chemical composition of CN/aerosols within the polar atmosphere remain open.

2. Laboratory Studies

The discussion of laboratory studies began with key questions being posed about the extent to which the systems created "indoors" and the fundamental processes studied there are relevant to the multiphase and complex systems known to exist "outdoors" in the real world. In recent years knowledge has clearly been developing about the varying characteristics of ice surfaces and the influence of temperature, humidity and the chemical composition of the atmosphere on their behaviors. It was concluded that such knowledge (and more) is essential for the design of appropriate laboratory experiments in order to advance the field.

The discussions covered both condensed-phase and gas-phase processes. Several wide-ranging points emerged, particularly regarding heterogeneous aspects:

- Gas/surface uptake partition coefficients should be measured especially for snow, brine and sea ice. Is frozen sea water a good proxy in this regard? There will be benefits to studying a simplified system, i.e. synthetic sea salt without the biotic components, but when do such media become irrelevant?

- Rate coefficients for fundamental reactions thought to be important (e.g. high ionic strengths in solution) should be measured. The experiments must be performed at low temperatures and as a function of temperature.

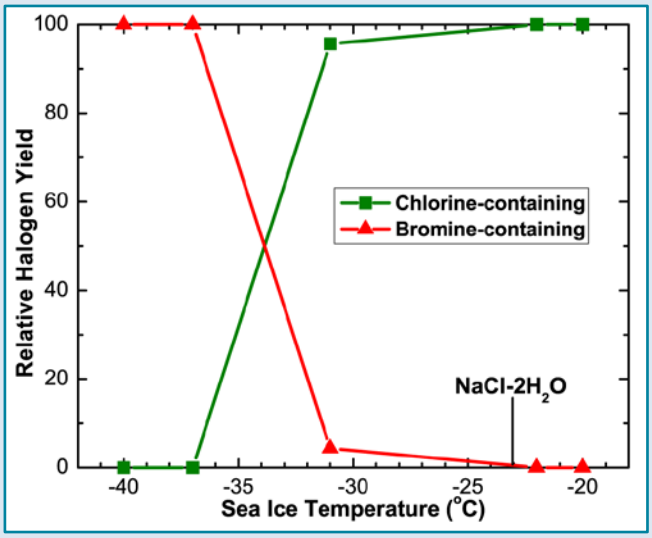

This figure shows the relative halogen product yields observed upon reaction of N_2O_5 with authentic sea ice surfaces versus temperature. Chlorine-containing products (squares) were dominated by $ClNO_2$ while bromine-containing products (triangles) included $BrNO_2$ and Br_2. The transition from chlorine- to bromine-dominated products with decreasing temperature is consistent with a strongly increasing bromide-to-chloride ratio in the ice-phase. The ratio increases due in part to preferential precipitation of chloride salts such as $NaCl\text{-}2H_2O$ at -23°C. The absolute halogen yield was always greater than 25%. (*Courtesy of J. P. Kercher and J. A. Thornton, University of Washington, Seattle, WA, USA*)

- Air/ice partition coefficients need to be measured for a variety of species; our knowledge of the surface characteristics of ice suggests it is probable that Henry's Law is not appropriate.
- Rates obtained in aqueous solutions should be compared with those measured in solids and, whenever possible, quasi liquid layers.
- What condensed phase reactants are really important? A little-studied question is whether or not there exist important reactions involving metals, e.g. Fe, Cu, Mn.
- Rate coefficients and product distributions at low temperatures for gas phase reactions should also be measured. Researchers should be aware of the existence of adducts/complexes at low temperatures when interpreting mechanisms.
- The uptake of $Hg_{(g)}$ on representative solids should be investigated, at any convenient concentrations. "Cold mercury" chemistry remains a big unknown in our knowledge base.

3. Shared Facilities

All agreed that there would be substantial merit in performing collaborative research experiments using ice surfaces generated in large reaction chambers. This was an important conclusion reached by the Workshop group. The questions are: How? Where? What should it be used for?

Enthusiasm was so great for this idea that potential configurations of a specialized chamber were discussed, e.g. frozen sea water with a cold air Teflon dome over it. In such a chamber, different surfaces (including frost flowers, synthesized snow etc.) could be tested, prepared, and utilized. Working toward the establishment of such a community ice chamber facility would bring together the laboratory, field and modeling communities in a realistic and productive way.

4. Coordinated/Scientifically Focused Field Experiments

The discussions centered on issues that could be best addressed by coordinated field experiments. Again one purpose of the Workshop was to pose questions and the following were deemed of most importance in this debate:

- What organic substrates are important in snow/sea ice? In fact, the fundamental question was raised: Do organics matter at all?
- Controlled field experiments to measure the relative rates and distribution of products of activation processes are required, e.g. from N_2O_5, RX, O_3, HOX.
- Fluxes above/to various surfaces of importance must be measured. There was considerable discussion about the need to measure fluxes of a wide variety of species, including inorganic materials and organic compounds such as OVOCs.
- The mechanisms for sea salt aerosol generation should be determined, e.g. sublimation of wind-blown frost flowers and blowing snow.

5. Data exchange, evaluation and assessment

It was agreed that communication between laboratory and polar field researchers was not altogether absent but that considerable effort is needed to maintain and enhance the relationship. Therefore the discussion centered on methods of improving information exchange, with an eventual aim to provide a proper

climate assessment study.

- Is there scope for improvement of communication between laboratory personnel, field workers and modelers, e.g, by data archiving and data evaluation?
- Is the field mature enough to embark on model assessment of the impact of pollution and climate change on the polar boundary layer processes?

6. Modeling

A need was identified to greatly improve mathematical modeling studies of ice-atmosphere processes on a wide range from the molecular scale (including molecular dynamics simulations) to the prediction of large scale atmospheric impacts. In particular molecular scale models of the quasi liquid layer (QLL) as a function of temperature were needed to answer the following important unknowns:

- What is the composition of QLL? Many technological difficulties are associated with this question as mentioned above but "simple" questions such as, 'Do all non-water species found in molten snow reside in the QLL?' remain to be answered.
- Can reactions in the QLL be modeled as in droplets? (If yes – above which critical QLL thickness is this not valid? If no – is Henry's law valid for QLL uptake? If not, what is a valid model?)
- Are currently used models valid for the QLL?
- How do quantum yields in the QLL compare with those in solid ice/bulk liquid?
- What chemistry happens at the QLL/substrate interface?

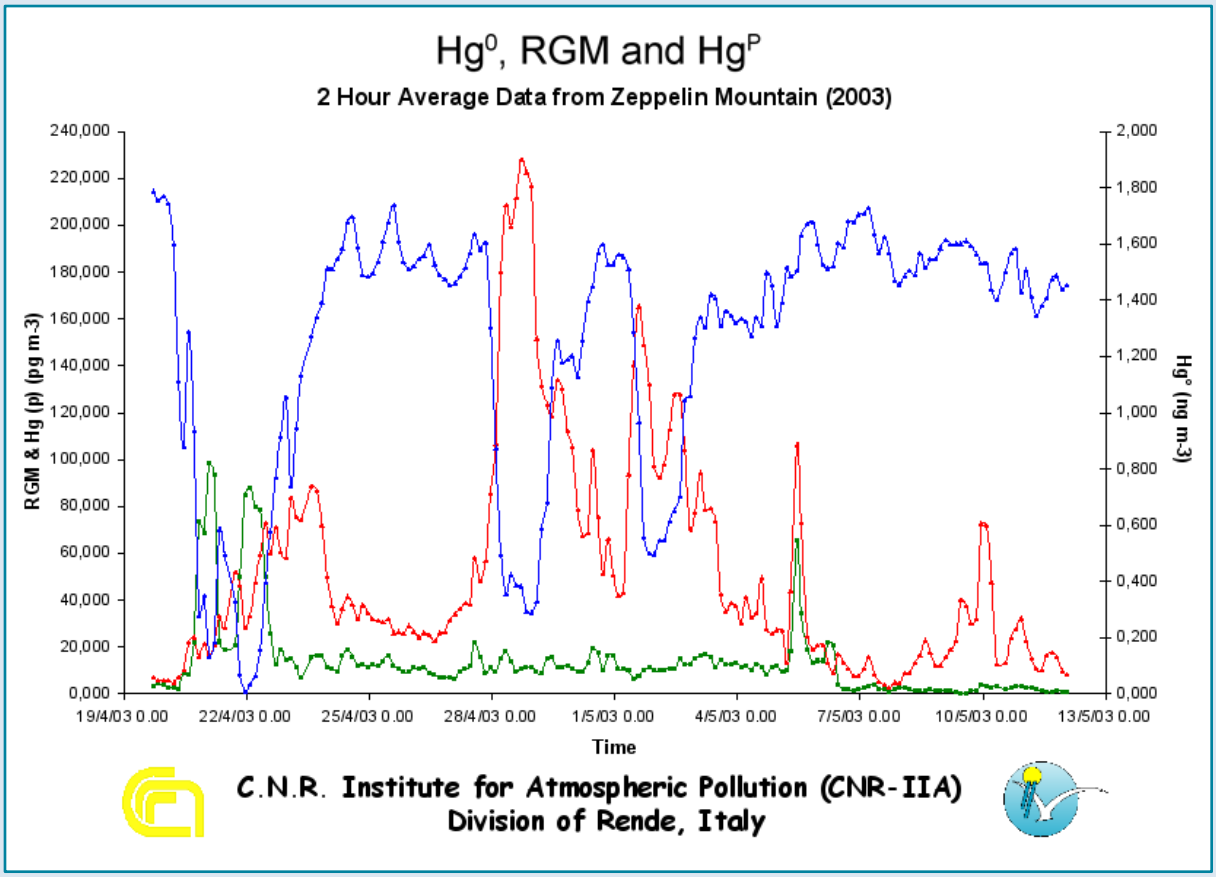

Atmospheric concentrations of elemental mercury (Hg_0, blue), Reactive Gaseous Mercury (RGM, red) and mercury associated with particulates (Hg_p, green) measured on Mt Zeppelin (Ny-Ålesund, Svalbard) during the MEDEX project in Spring 2003. The three pronounced periods of extremely low elemental mercury can be clearly seen, and it is also clear that these periods are at times accompanied by high concentrations of RGM (an operational definition referring to gas phase oxidized Hg compounds which can be sampled using a KCl denuder), but that this is not always the case. (*Modified from Sproveiri et al., 2005, Figure 6*)

In true Workshop fashion it was also suggested that these were the wrong questions to ask! The main issues might simply be those relevant to other parts of the atmosphere. Hence detailed knowledge of the QLL may be irrelevant, and instead what is needed is reaction rate and total uptake data. The QLL might be regarded simply as a solid phase/surface issue and not necessarily involved in the "dirty", liquid, chemistry present at the poles. These issues were not resolved although it was concluded that interfacial kinetics could not be properly represented by parameters simply transferred from the bulk liquid phase.

Other modeling issues were also discussed:

- $CaCO_3$ precipitation and temperature-dependence of critical equilibrium warrants more study; experiments are particularly required to test the models.
- What is the importance of frost flowers? A source function/parameterization for inclusion in local and global models is required, similar to that recently reported for blowing snow.
- Better modeling of the fluxes of key gases relevant to field monitoring is needed.
- A detailed kinetics model of the life cycle of atmospheric mercury species, including gas-phase and condensed (ice) reactions is required.

AICI : Where next?

The scientific objectives of AICI have always linked directly to two over-arching science questions posed for/by IGAC, namely:

- Within the Earth System, what effects do changing regional emissions and depositions have on air quality and the chemical composition of the planetary boundary layer?
- What is the role of atmospheric chemistry in amplifying or damping climate change?

The corresponding questions for answer in AICI have been:

- How will changing amounts of sea ice, snow cover, and atmospheric ice alter atmospheric chemistry and composition? Are there important feedbacks to climate?
- What are the present regional emissions and losses over snow, ice and sea ice? How could they alter with changing climate?

It was clear from the workshop discussions we do not yet have enough quantitative information and understanding of basic parameters for predictive numerical models to help answer the AICI questions. This is particularly true of chemical processes occurring at the air/ice interface and the physical processes involved in the production and loss of atmospheric particulate material. This leads to large uncertainties in the source terms for reactive gases (halogens, NO_x species, Hg, etc.) and recycling of these gases in the polar environment.

To help us move forward, the AICI community concluded that it would be worthwhile considering coordinated laboratory/chamber studies in order to address questions such as:

- What is the composition of ice?
- Do impurities sit on the surface?
- What type of layer do the impurities sit in and how fast do they form?
- What are the chemical and physical natures of the QLL and QBL?
- How are 'sea salt' aerosols produced over ice-covered zones?
- How much recycling of reactive species occurs in the snow and the aerosol?
- What is the role of condensed-phase photo-chemistry?

Hence we need to invest in a community-based/-accessible cold surfaces reaction chamber of sufficient volume to enable study of a range of surfaces and to simultaneously measure reaction products. This effort is crucial because it is important to relate what is measured in the laboratory to the real outdoor environment and *vice versa*. AICI should act to initiate the coordination of this effort and in due course organize a major conference to publicize the results achieved in this fascinating aspect of Atmospheric Science.

Acknowledgments

In order to reach the Workshop targets, some finance was, of course, required to invite both speakers and "Young Scientists"; for that, the assistance of IGAC, BAS and ESF-INTROP is gratefully acknowledged. The on-site help of a number of people at BAS, most particularly Anna Jones, as co-organizer of this event is particularly acknowledged.

References

Schönhardt, A., A. Richter, F. Wittrick, H. Kirk, H. Oetjen, H. K. Roscoe and J. P. Burrows, Observations of iodine monoxide columns from satellite, *Atmos. Chem. Phys.*, **8**, 637-653, 2008.

ACPD Special Issue Articles

Anderson, P. S. and W. D. Neff, Boundary layer physics over snow and ice, *Atmos. Chem. Phys.*, **8**, 3563-3582, 2008.

Anderson, P. S. and W. D. Neff, Corrigendum to "Boundary layer physics over snow and ice" published in Atmos. Chem. Phys., 8, 3563–3582, 2008, *Atmos. Chem. Phys.*, **8**, 4115-4115, 2008.

Domine, F. et al., Snow physics as relevant to snow photochemistry, *Atmos. Chem. Phys.*, **8**, 171-208, 2008.

Grannas, A.M. et al., An overview of snow photochemistry: evidence, mechanisms and impacts, *Atmos. Chem. Phys.*, **7**, 4329-4373, 2007.
Simpson, W. R. et al., Halogens and their role in polar boundary-layer ozone depletion, *Atmos. Chem. Phys.*, **7**, 4375-4418, 2007.
Steffen, A. et al., A synthesis of atmospheric mercury depletion event chemistry in the atmosphere and snow, *Atmos. Chem. Phys.*, **8**, 1445-1482, 2008.

Announcements

Joint CACGP / IGAC Conference

July 6-10, 2010




Joint CACGP / IGAC Conference

July 6-10, 2010

Halifax, Canada

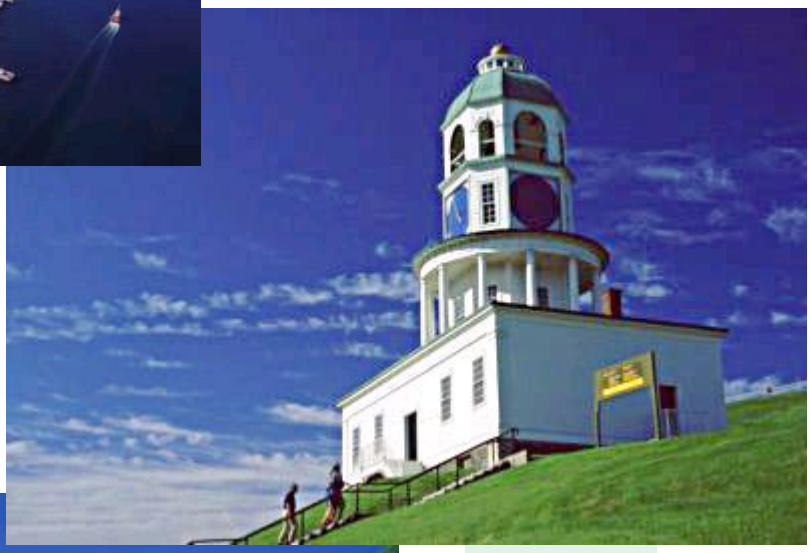

Please help us keep our mailing list up to date by sending your revised contact information:

IGAC Core Project Office
NOAA-PMEL
7600 Sand Point Way
Seattle, WA 98115-6349 USA

email: igac.seattle@noaa.gov

IGACtivities Newsletter

Editor: Sarah Doherty
Production manager: Ho Ching Lee
Newsletter formatting: Beth Tully
IGAC logo: Linda Kubrick

Published by IGAC Core Project Office
RESEARCH CENTER FOR ENVIRONMENTAL CHANGE
ACADEMIA SINICA
128 Academia Rd. Sec. 2
P.O. Box 1-55 NanKang
Taipei, 11529 Taiwan

臺灣郵政台北誌字第 137 號執照登記為雜誌交寄
發行人：劉紹臣
發行所：中央研究院環境變遷研究中心
發行地址：台北市 115 南港區研究院路二段 128 號 1-55 號信箱

IGAC was initiated by the Commission on Atmospheric Chemistry and Global Pollution (CACGP) and is a Core Project of the International Geosphere-Biosphere Programme (IGBP). The IGAC Seattle Core Project Office is currently supported by the National Science Foundation (NSF), National Aeronautics and Space Administration (NASA), and National Oceanic and Atmospheric Administration (NOAA). The IGAC Taipei Core Project Office is funded by Academia Sinica, Taipei. The Rome Core Project Office is supported by the Italian National Research Council and by the European Commission Network of Excellence ACCENT. Any opinions, findings and conclusions, or recommendations expressed in this newsletter are those of the individual author(s) and do not necessarily reflect the views of the responsible funding agencies.

IGACtivities Newsletter

Taipei TAIWAN

R.O.C.

POSTAGE PAID

NEWSLETTER
LICENCE NO.N285

國內
郵資已付

台北郵局許可證
台北字第 285 號

IGAC Core Project Office
RESEARCH CENTER FOR ENVIRONMENTAL CHANGE
ACADEMIA SINICA
128 Academia Rd. Sect. 2
P.O. Box 1-55 NanKang
Taipei, 11529 Taiwan

Printed on Recycled Paper

Please Recycle after Use!